GEOCHEMICAL CHARACTERISTICS OF THE LOWER MESOZOIC SEDIMENTS IN THE MOUNT FREELING AREA, NORTHWESTERN FLINDERS RANGES

Thesis submitted in accordance with the requirements of the University of Adelaide for an Honours Degree in Geology

Farid Shahin

November 2012

THE UNIVERSITY of ADELAIDE

TITLE

Geochemical characteristic of the lower Mesozoic sediments in the Mount Freeling area, northwestern Flinders Ranges.

RUNNING TITLE

Geochemical characteristics of Mount Freeling

ABSTRACT

An increased resource demand is largely due to the exhaustion of mineral deposits that are from predominantly shallow exposed settings, hence, in Australia there is a growing need for exploration techniques that provide an improved understanding of areas of deep transported cover. A case study conducted on lower Mesozoic sediments overlying the Mount Painter Inlier, NW Flinders Ranges (Mount Freeling area), using combined geochemical analysis, detrital zircon provenance data and Hylogger data aims to understand the source and characteristics of the transported cover. The Mount Painter Inlier consists of predominantly Mesoproterozoic sedimentary rocks and granites. Neoproterozoic sedimentary and volcanic sequences of the Adelaide Fold Belt form a cover up to 14km thick, therefore making the overlying lower Mesozoic sediments appropriate for refining the combined exploration techniques. Hylogger core scans conducted on the Recorder Hill, Ludbrook and Trinity Well Type Sections, NW of Mount Painter Inlier, show increases in the degree of crystallisation of kaolinite implying more proximal source regions moving stratigraphically up the profiles. U–Pb dating of detrital zircons shows a maximum depositional age of 122 Ma and 400 Ma for the Ludbrook and Recorder Hill samples respectively with the most influential sources being the Mount Painter Inlier and the Gawler Craton. HyLogger and Zircon data suggest that where there is a higher degree of crystallisation, there is a younger maximum depositional age and vice versa. The geochemical data set shows that when A-CN-K plots are used to plot the degree of feldspar weathering, samples tend to fall into groups and then these sub-groups can be used to recalculate anomalous and background levels for trace elements and major elements. Through the use of geochemistry, HyLogger and detrital zircon studies it has been shown that mineralisation zones can be targeted more cost effectively and efficiently.

KEYWORDS

Geochemical, Flinders Ranges, Mount Freeling, HyLogger, Detrital Zircon, Lower Mesozoic, Regolith, Deep Basin, Geochronology, Sediment Provenance

TABLE OF CONTENTS

LIST OF FIGURES AND TABLES

1. INTRODUCTION

In Australia there is a growing interest in the development of exploration techniques to better consider areas of deep transported cover. This is largely due to the increasing demand on resources having near exhausted existing mineral discoveries that have mostly come from shallow exposed settings. The northwest Flinders Ranges provides a case study context for the development of new exploration methods. The area has a thick transported sediment cover that masks the bedrock geochemical signatures. Most of the work in the area has been stratigraphic and has focused on sedimentary type sections. To date there have been no in depth geochemical characterisation studies conducted on these sections, nor any detrital zircon studies to determine the provenance and depositional age of these sediments and HyLogger core scans through the area. Therefore, an important component of their physical and chemical dispersion system remains unknown.

The case study area for this investigation lies to the northwest of the Mount Painter Inlier, which mostly consists of Mesoproterozoic sedimentary rocks and granites that contain an abundance of U and Th (Wülser *et al.* 2011). Two initial subject areas were selected from previous literature and a third was agreed upon while in the field that had only recently been made visible due to recent high rainfall and stream discharge. The Trinity Well Type Section at Western Spur and the Recorder Hill Type Section on the prominent rise, informally referred to as 'Recorder Hill' were the two pre selected type sections. The third section near Pelican Well, was initially described by Ludbrook (1966) but since has been further eroded and better exposed in recent years and, therefore had not been previously described and interpreted in detail.

The bedrock geology is mostly buried beneath a thick, transported sedimentary layer sequence that may conceal and dilute the geochemical expression of mineral systems, but may also reaccumulate and spread the geochemical expression of mineral systems thereby providing an enlarged exploration target. Although the wider geochemical dispersion of elements can have advantageous, understanding the distal footprints of reworked and diluted mineral systems and their contributions to sedimentary systems is a major challenge. For this reason developing a better understanding of the geochemical characteristics of sedimentary systems for mineral exploration is a major research and mineral exploration frontier.

This study aims to fill in the gap of knowledge specifically for the Mount Freeling area by geochemically characterising type sections of the basal (Mesozoic) Eromanga Basin sediments, conducting a provenance detrital zircon study on two of the stratigraphic units in order to constrain the provenance of the sediments, as well as undertaking in-depth lithological logging and scans of the type sections using HyLogger core scanner. This will highlight the relationship between the geochemical signatures of bedrock mineralisation and the buried sediment expressions of mineralisation. This will enable the characterisation of lithological and stratigraphic units, and to determine what can be considered background and elevated geochemical levels for different components of the deep sedimentary cover section, that can be further extrapolated to other exploration areas.

2. BACKGROUND

The Mount Painter Province was geologically mapped through the early 1960s, and then published in 1969. This study will focus along the NW margin of the map area (Australia 1969). The three type sections that this study focuses on are:

1. The Recorder Hill Type Section at a site informally referred to as 'Recorder Hill'(GDA: 322689mE 6691559mN);
2. The Trinity Well Type Section at Western Spur (GDA: 335465mE 6697106mN); and,
3. The Ludbrook Type Section near Pelican Well (GDA: 320944mE 6686841mN).

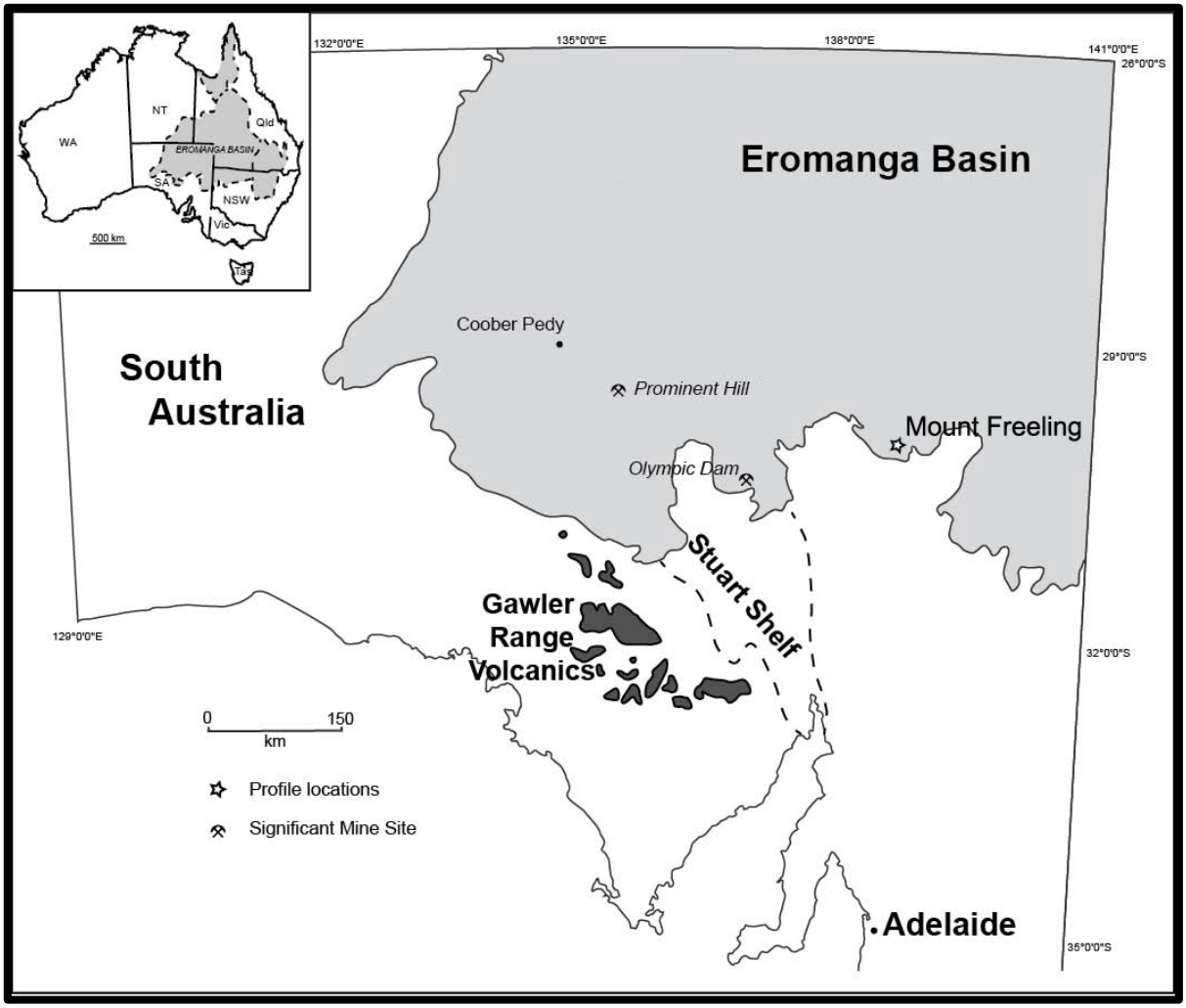

Figure 1: Location map showing the Mount Freeling study area. Modified from Dart and Hill (2012).

2.1 Geological Setting

The Mount Painter Province mostly consists of Mesoproterozoic sedimentary rocks and granites (Armit *et al.* 2001). Prior to the deposition of the Neoproterozoic sedimentary and volcanic sequences of the Adelaide Fold Belt in the area, the sediments and granites underwent two stages of deformation. Later burial by the Adelaidean sediments and volcanics is estimated to be up to 14 km thick (Teale 1993), with deposition over a ~350 million year period eventually coming to an end with the onset of the Delamerian Orogeny (Foden *et al.* 2006, Wülser *et al*. 2011).

The basin that is the focus of this study is the Eromanga Basin, a Mesozoic intracratonic sag basin (Gravestock *et al.* 1986), that covers an area of approximately to a million square kilometres spanning most of east-central Australia (Skirrow 2009). The Eromanga Basin has been subdivided into three major units corresponding to changes in depositional environment and further correlated to the timing of the deposition. The three major sequences of the Eromanga Basin are:

1. A lower non-marine sequence deposited in the early Jurassic to earliest Cretaceous (Algebuckina Sandstone);
2. A middle marine sequence from the early Cretaceous (Cadna-owie Formation and Bulldog Shale); and,
3. An upper non-marine sequence from the late Cretaceous (Winto Formation) (Skirrow 2009).

The lower non-marine sequence consists mostly of medium-grained sands deposited in a fluvial environment. This is followed by the middle sequence consisting of fine-

grained lacustrine sands, silts and shales (Drexel *et al.* 1995, Skirrow 2009). The upper non-marine sequence is referred to as the Winton Formation. This study will not focus on this upper layer as it does not occur in the greater area of the Frome Embayment and the study area. The middle marine sequence includes a basal, marginal marine, sand unit, referred to as the Cadna-owie Formation (Skirrow 2009). Within the larger area of the Frome Embayment the Cadna- owie Formation is prograding into deeper water, shales and muds. Still within the middle marine sequence, but overlying the Cadna-owie Formation, is the Cretaceous Bulldog Shale. The Cretaceous Bulldog Shale is the capping layer of the Eromanga Basin in this field area, described as blue-grey silty clay when fresh (Ellis 1976).

Overlying the Eromanga Basin is the Cenozoic Lake Eyre Basin. This basin was created during the late Paleocene tectonic subsidence. This was followed by episodic fluvial and lacustrine sedimentation continuing through the basin until present day (Callen *et al.* 1995, Skirrow 2009). The Eyre Formation of the Lake Eyre Basin is the basal fluvial unit that unconformably overlies the Eromanga Basin. This occurs as a capping to the Trinity Well type section at Western Spur.

2.2 Previous Studies

The Mount Freeling area in the northwestern Flinders Ranges poses a mineral exploration challenge typical of many parts of Australia and the world. The bedrock is buried, and therefore at first glance obscured, by a thick sequence of sediments. The specific problem for mineral explorers in these areas is that the vertical dispersion of indicator elements of mineral systems through the sediment pile towards the land surface is restricted and therefore not readily accessed in exploration programs (Butt *et*

al. 2000, Anand 2005). Generally the geochemical expressions become masked and/or diluted by geochemical and mechanical processes that have occurred within the sediments throughout their geological history. Instead the sediments are often "swamped" by the geochemical expression of the bedrock from adjoining areas, such as the basin hinterland (Anand and Robertson 2012). The most direct way to overcome this issue of transported thick basin cover is to go through the difficult operation of deep drilling through the transported cover, however, this is both expensive and time consuming. There have been a number of discussions on how geochemical detection vertically through thick, transported deeply weathered sediments in arid terrains is not successful and no single model of how this may be achieved has been widely accepted (Smee 1998, Gray *et al.* 1999, Kelley *et al.* 2003).

In Australia and many other parts of the world there is a greater push for exploration techniques to move into areas of deep transported cover, where sediment thicknesses are greater than 30 m. This is due to more easily accessible areas of mineralisation becoming exhausted (Anand and Robertson 2012), due the cost of deep drilling no longer being an affordable and time effective technique.

In an attempt to understand thick sedimentary cover geochemistry in Australia, a firm understanding of Australia's complex erosional and depositional history, past climates, and weathering patterns must be taken into account. This includes overprinting and reworking of events at multiple localities through the transportation history of sediments. The Mount Freeling/Mount Painter region has a sedimentary cover sequence that is hundreds of meters thick. Very little research has been done on these sediments

to try and determine their provenance and whether these sediments are able to provide a signature for the proximal bedrock or potentially any buried mineralisation. Overprinting from weathering and induration has complicated the geochemical signature preserved in these sediments. The key complication in recent geological times is that the Mount Painter Province has been subjected to high intensity weathering and erosion (Coats and Blissett 1971) over long (>200 Ma) geological timeframes.

Previously the Mount Freeling area has been examined in depth by Alley (1987, 1993, 1998), Franks (1991, 1995) and Forbes (1982). With an absence of publications for nearly a decade, Alley and Franks co-authored a paper in 2003 that presented evidence of Mesozoic glaciation in the northwest Flinders Ranges area. Near the base of the Eromanga Basin, at Trinity Well, a diamictite (assigned the name Livingston Tillite Member of the Cadna-owie Formation) was identified, indicating a glaciation occurred in the northern Flinders Ranges during the Early Cretaceous (Alley and Frakes 2003). The stratigraphy of the area has been documented in detail through research mapping in the 1960s, providing an account of the stratigraphy and the interpreted depositional environment for these sediments. The Cadna-owie Formation has been broadly described as a partly carbonaceous, fine to medium grained sandstone deposited under shallow water, marginal-marine conditions (Forbes 1982, Alley 1987). The Bulldog Shale is documented as a bioturbated, fossiliferous, carbonaceous, silty claystone containing minor sandstone deposited in marine conditions (Alley 1987). Isolated boulders and minor gravel layers, sourced from the including Gawler Range porphyry and Devonian quartzites, are common in the shales with greater concentrations occurring towards the base of the unit (Ludbrook 1966, Flint *et al.* 1980).

A major gap in geological knowledge of basin sediments in the northwest Flinders Ranges and more specifically the Mount Freeling area is the lack of whole-rock geochemistry to accompany the already well described type sections in the area. This in turn will allow assessment of whether geochemical expressions of locally buried or regionally derived bedrock and possible mineral systems can be detected and further studied and potentially correlated to other anomalies across the wider basin. A further major gap in knowledge is a firm understand of where the transported sediments deposited in the area have originated from. This is to be addressed with detrital zircon dating of two units that have been picked due to their high zirconium levels. The results from this will be linked back to provenance bedrock lithologies and supported by HyLogger core scans.

3. METHODS

3.1 U-Pb zircon LA-ICP-MS geochronology

Analytical techniques for U-Pb isotopic dating of zircons follow those of Payne *et al.* (2006) and Howard *et al.* (2009). Samples from the Mount Freeling area were cleaned of weathered material and potential contaminates under water with a sterile wire brush, pieces were broken down with a mallet or rock saw where necessary to less than 2 cm x 7 cm x 15 cm and passed through the jaw crusher. The crushed rock was then sieved with the 79-425 μm fraction collected for the concentration and extraction of zircons. The sieved fraction was then panned to remove more unwanted grains. This is an effective process as zircons are heavy minerals that through the panning process will reside at the bottom allowing all the lighter material to be washed away. The heavy minerals collected during panning were then dried.

Magnetic minerals were removed from the heavy mineral samples by multiple Frantz passes, slowly increasing the intensity of the magnetic field with each pass to avoid overloading the machine. Once the magnetic materials have been removed, the samples are then passed through heavy liquids. Zircon grains are then handpicked and mounted into a 2.5 cm diameter circular epoxy resin block and hand polished until the centre of the zircons are revealed. All grains were cathodoluminescence (CL) imaged using a Phillips XL-20 scanning electron microscope. The U–Pb isotopic analyses were obtained using a New Wave 213 nm Nd-YAG laser in a He ablation, coupled to an Agilent 7500cs ICP-MS at the University of Adelaide, Adelaide Microscopy facilities. The laser spot diameter used was approximately 30 μm at the sample surface with a repetition rate of 5 Hz.

Raw LA-ICP-MS data were processed using 'GLITTER', a data reduction program developed at Macquarie University, Sydney (Griffin *et al.* 2008). U–Pb fractionation was corrected using the GJ zircon (TIMS normalisation data $^{207}Pb/^{206}Pb$=607.7 ± 4.3 Ma, $^{206}Pb/^{238}U$ age = 600.7 ± 1.1 Ma and $^{207}Pb/^{235}U$ age = 602.0 ± 1.0 Ma (Jackson *et al.* 2004)). Accuracy was checked with Plešovice zircon standard mean (ID-TIMS $^{207}Pb/^{206}Pb$ U-Pb age of 337.13 ± 0.37 Ma (Sláma *et al.* 2008). Throughout the study, the weighted averages obtained for GJ were $^{207}Pb/^{206}Pb$= 608.2 ± 4.9 Ma (n=155, MSWD=0.29) and $^{206}Pb/^{238}U$= 600.4 ± 1.2 Ma (n=155, MSWD=0.66). Plešovice are $^{207}Pb/^{206}Pb$= 336.7 ± 5.9 Ma (n=44, MSWD=0.94) and $^{207}Pb/^{235}Pb$= 336.5 ± 3.1 Ma (n=44, MSWD=1.2).

3.2 Whole rock geochemistry

An approximate 250g representative sub-sample was taken from each bulk sample obtained in the field for geochemical analysis by Acme Laboratories, Vancouver, Canada. Element analysis was conducted for the following elements: Ba, Be, Co, Cs, Ga, Hf, Nb, Rb, Sn, Sr, Ta, Th U, V, W, Zr, Y, La, Ce, Pr, Nd, Sm, Eu, Gd, Tb ,Dy, Ho, Er, Tm, Yb, Lu, Mo, Cu, Pb, Zn, Ni, As, Cd, Sb, Bi, Ag, Au, Hg, Tl, Se, SiO_2, Al_2O_3, Fe_2O_3, CaO, MgO, Na_2O, K_2O, MnO, TiO_2, P_2O_5, Cr_2O_3. Elements were analysed by XRF (major elements) and ICP-MS (REE and trace elements). All samples were pulverised to >80% passing 200 μm mesh. Whole rock XRF preparation was by $LiBO_2$ fusion of a 12 g sample pulp. ICP-MS analysis preparation was by a lithium metaborate / tetraborate fusion and nitric acid digestion for the REE and refractory elements and a aqua regia digest for precious and base metals. Measured elements and their detection limits from the above processes are provided in Table 1

XRF (Detection limit %)	ICP-MS (Detection limit ppm)
SiO_2 (0.1), Al_2O_3 (0.01), Fe_2O_3(0.01), CaO (0.01), MgO (0.01), Na_2O (0.01), K_2O (0.01), MnO (0.01), TiO_2 (0.01), P_2O_5 (0.01), Cr_2O_3, Ba (0.01), Tot/C (0.02), Tot/S (0.02)	Ba (1), Be (1), Co (0.2), CS (0.1), Ga (0.5), Hf (0.1), Nb (0.1), Rb (0.1), Sn (1), Sr (0.5), Ta (0.1), Th (0.2), U (0.1), V (8), W (0.5), Zr (0.1), Y (0.1), La (0.1), Ce (0.1), Pr (0.02), Nd (0.3), Sm (0.05), Eu (0.02), Gd (0.05), Tb (0.01), Dy (0.05), Ho (0.02), Er (0.03), Tm (0.01), Yb (0.05), Lu (0.01), Mo (0.1), Cu (0.1), Pb (0.1), Zn (1), Ni (0.1), As (0.5), Cd (0.1), Sb (0.1), Bi (0.1), Ag (0.1), Au (0.5 ppb), Hg (0.01), Tl (0.1), Se (0.5)

Table 1: Analytical method and detection limit for elements analysed by Acme Labs

3.3 HyLogger Core Scanner

The Hylogger Core scanner was developed by the CSIRO Mineral Mapping Technologies Group to provide detailed mineralogy of drill core. The Hylogger consists of a visible to short-wave infrared spectrometer (VNIR & SWIR), coupled with a linescan digital imager (Keeling *et al.* 2004). This wavelength range enables

identification of Al, Fe and Mn oxides and hydroxides, carbonates, sulphates and micas, but not silicate minerals. Representative sample chips of the Trinity Well, Recorder Hill and Ludbrook Sections were placed into black chip trays and scanned by staff at the Department for Manufacturing, Innovation, Trade, Resources and Energy (DMITRE). Data processing was undertaken using 'The Spectral Geologist' version 7 developed by CSIRO Australia; presentation of data was also produced through 'The Spectral Geologist' version 7.

4. OBSERVATIONS AND RESULTS

Three profiles have been sampled for this study and include: the Trinity Well type section; Recorder Hill type section; and, the Ludbrook reference section. The results presented below are grouped by section. Geochemical analysis was undertaken on samples from each profile, the complete raw analytical data are provided in Appendix 1. The whole suite of elements was not included for all samples, this is due to a portion of the data being from a historical data set. Two passes over each black chip tray was conducted. Due to both passes being near identical only one pass will be presented below and the complete HyLogger data presented in Appendix 2.

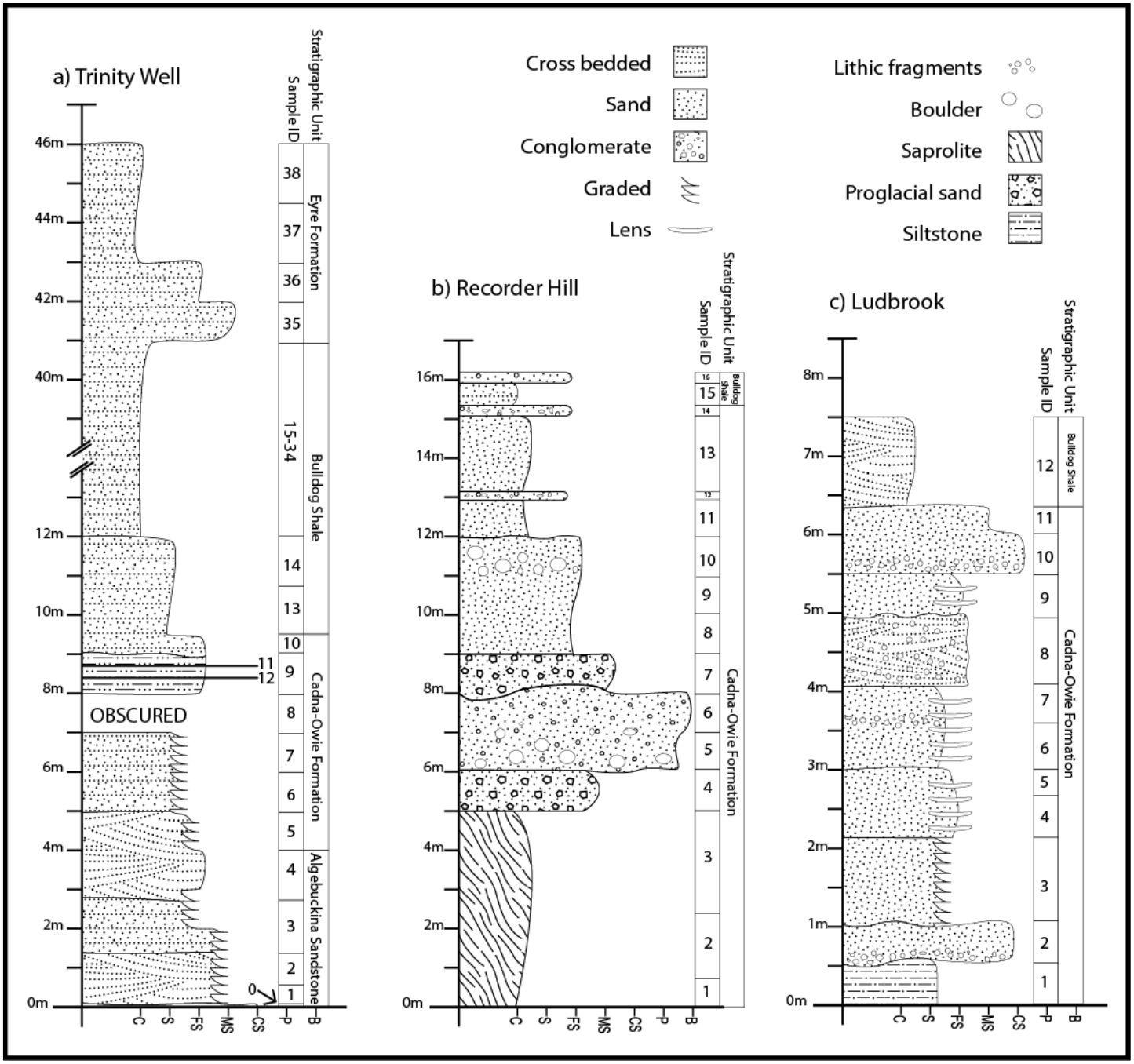

Figure 2: Stratigraphic logs of the Trinity Well, Recorder Hill and Ludbrook type sections at locations 322689mE 6691559mN, 335465mE 6697106mN and 320944mE 6686841mN respectively. Trinity well sample location 8 was obscured during April field visit and therefore has been left out of stratigraphic log. Samples were taken from each notable horizon change and this is identified as the Sample ID in the column adjacent to each log along with the stratigraphic unit for each sample point.

4.1 Recorder Hill

The Recorder Hill type section includes 16 sample points with a total of 18 samples taken due to 2 duplicates. A combination of geochemical analysis and HyLogger core scanner data was acquired for this type section. One sample was also chosen for detrital zircon provenance studies.

	Range	Minimum	Maximum	Mean	Std Dev.
SiO_2	65.30	26.90	92.20	63.67	17.74
Al_2O_3	13.17	3.65	16.82	8.27	4.01
Fe_2O_3	38.62	0.95	39.57	5.07	8.73
CaO	23.26	0.06	23.32	7.40	8.89
MgO	1.90	0.16	2.06	0.84	0.60
Na_2O	4.86	0.08	4.94	1.07	1.41
K_2O	2.82	0.36	3.18	1.68	1.02
MnO	3.49	0.02	3.51	0.24	0.82
TiO_2	0.59	0.27	0.86	0.54	0.20
TOT/C	5.32	0.00	5.32	1.72	2.02
TOT/S	0.63	0.00	0.63	0.16	0.20

Table 2: Summary statistics of major elements from the Recorder Hill type section. n=18.

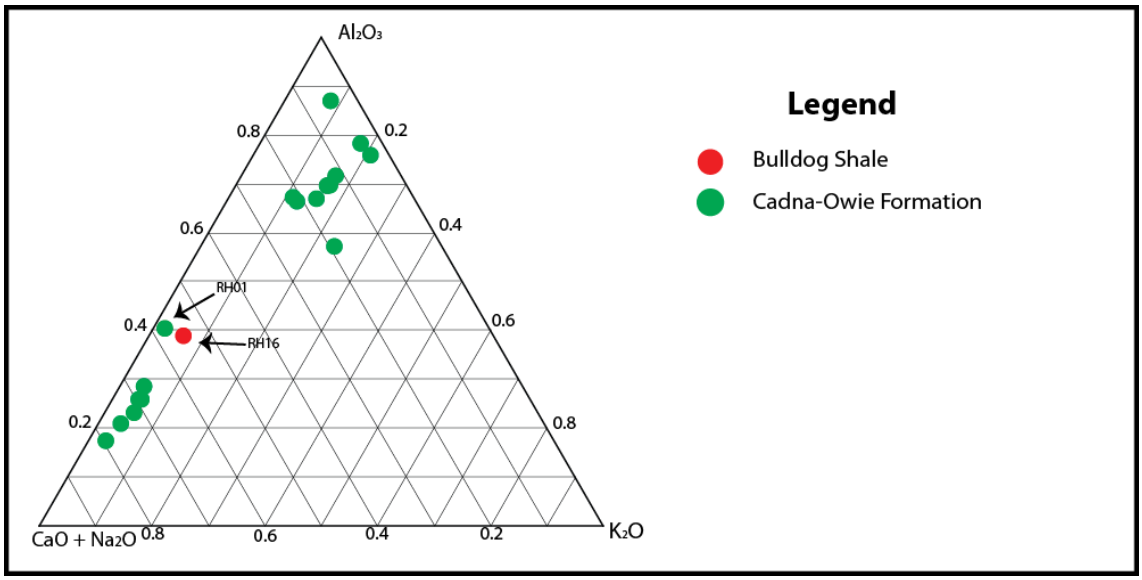

Figure 3: A-CN-K ternary plot of all samples from Recorder Hill type section.

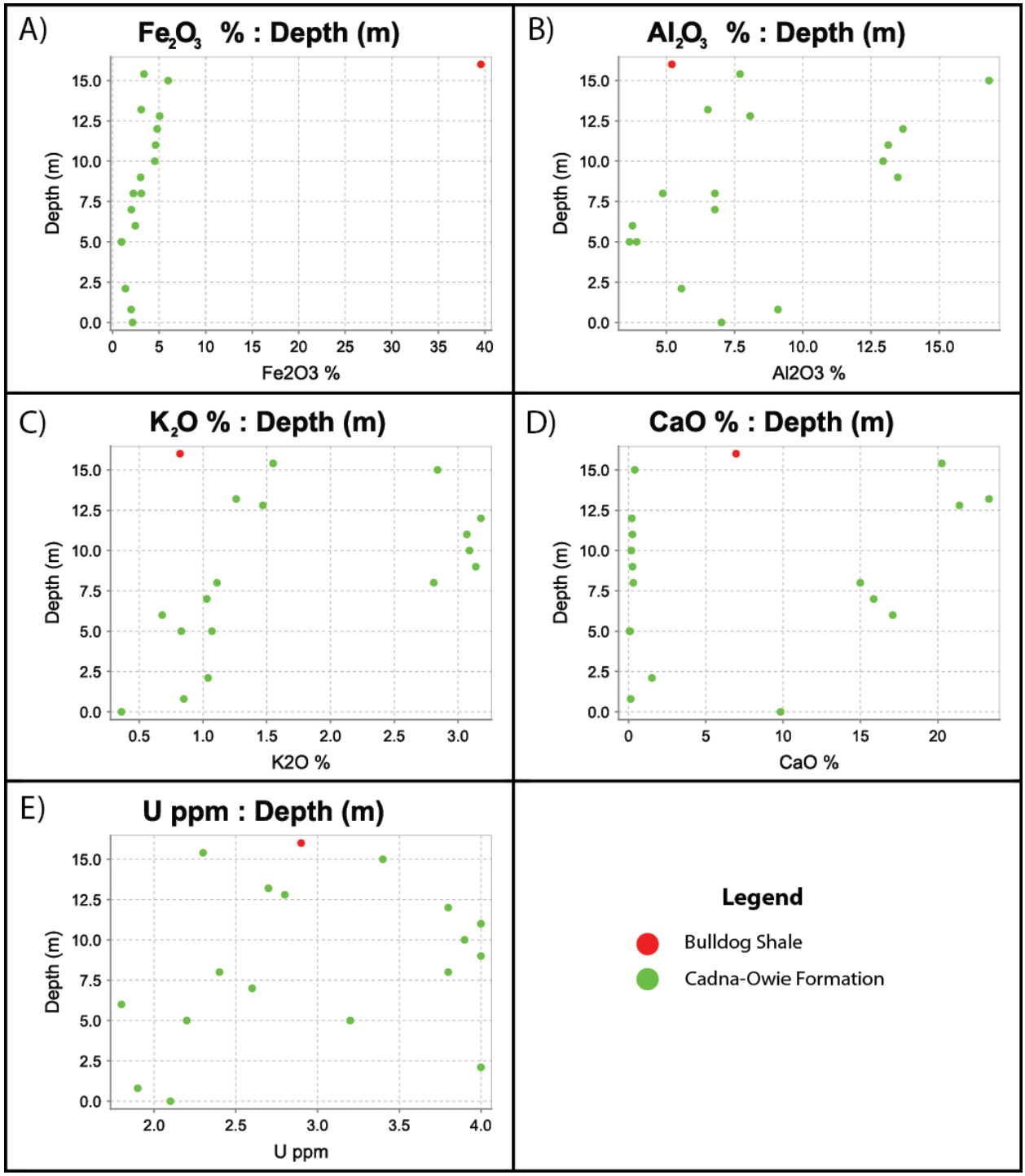

Figure 4: Down hole XY scatter plot of the Recorder Hill type section with depth (m) with respect to a) Fe_2O_3, b) Al_2O_3, c) K_2O, d) CaO and e) U.

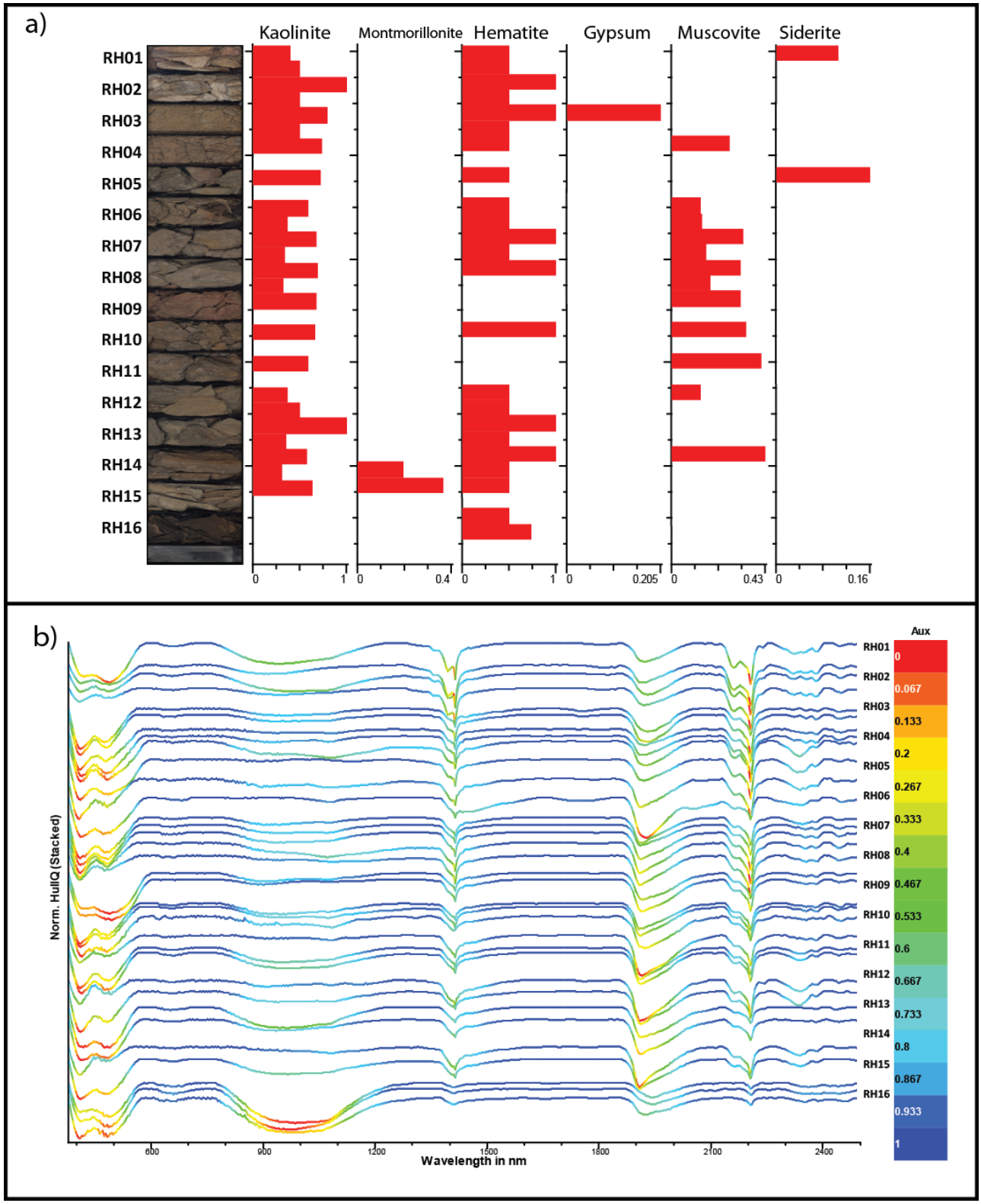

Figure 5: a) Recorder Hill type section HyLogger down chip tray interoperation produced via CSRIO The Spectral Geologist 7.0 for the first of two passes showing relative amounts of various minerals with corresponding photo of the sample in the black chip tray. b) All spectral signatures stacked for the first of two passes with corresponding sample ID.

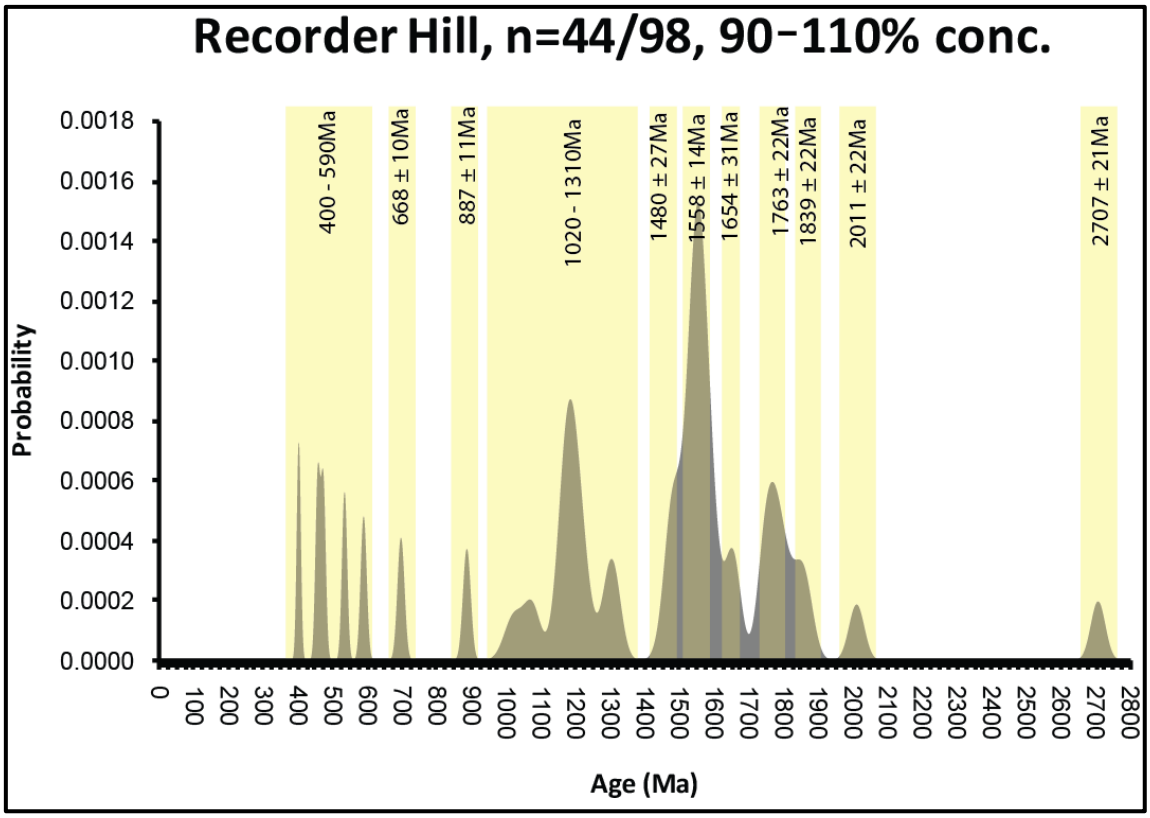

Figure 6: Probability density plot of all 44 within 10% concordant zircon analysis from 98 analysis conducted. Unique ages and age domains highlighted showing a wide spread of ages within sample RH04.

4.2 Trinity Well

The Trinity Well Type Section includes 39 sample points with 1 duplicate sample totalling 40 samples. All 40 samples were geochemically analysed and 39 samples were passed through the HyLogger.

	Range	Minimum	Maximum	Mean	Std Dev.
SiO_2	90.70	7.50	98.20	71.73	21.05
Al_2O_3	34.46	0.28	34.74	9.77	7.67
Fe_2O_3	66.18	0.04	66.22	8.00	15.07
CaO	2.53	0.03	2.56	0.34	0.55
MgO	1.35	0.01	1.36	0.32	0.34
Na_2O	2.19	0.02	2.21	0.64	0.71
K_2O	8.67	0.03	8.70	0.92	1.38
MnO	0.23	0.00	0.23	0.02	0.04
TiO_2	1.28	0.05	1.33	0.63	0.29
TOT/C	0.00	0.12	0.12	0.12	0.00
TOT/S	0.00	0.15	0.15	0.15	0.00

Table 3: Summary statistics of major elements from the Trinity Well type section n=40.

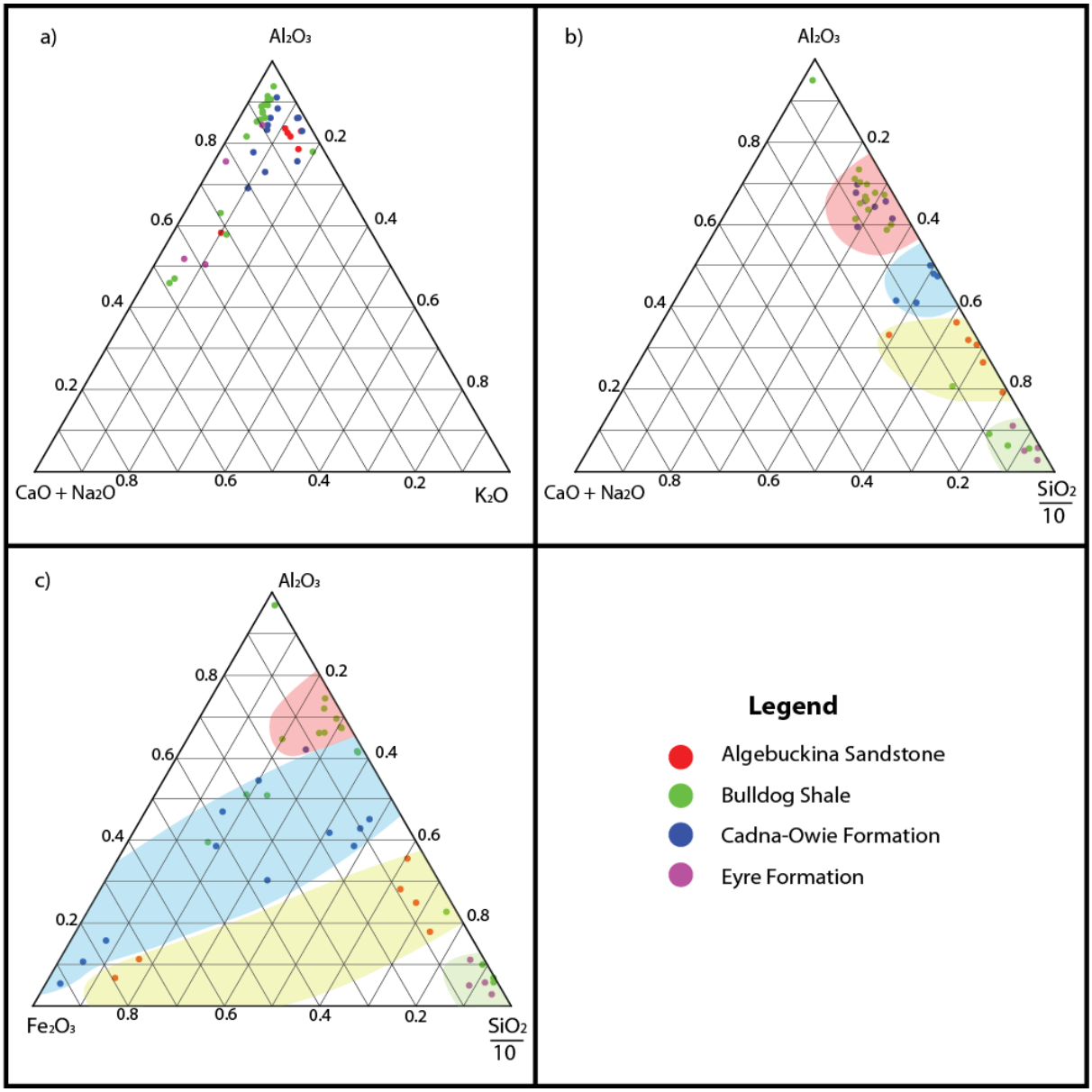

Figure 7: Ternary plots of all Trinity Well samples including two duplicate samples. a) A-CN-K ternary plot, b) A-CN-Si ternary plot and c) A-Fe-Si ternary plot.

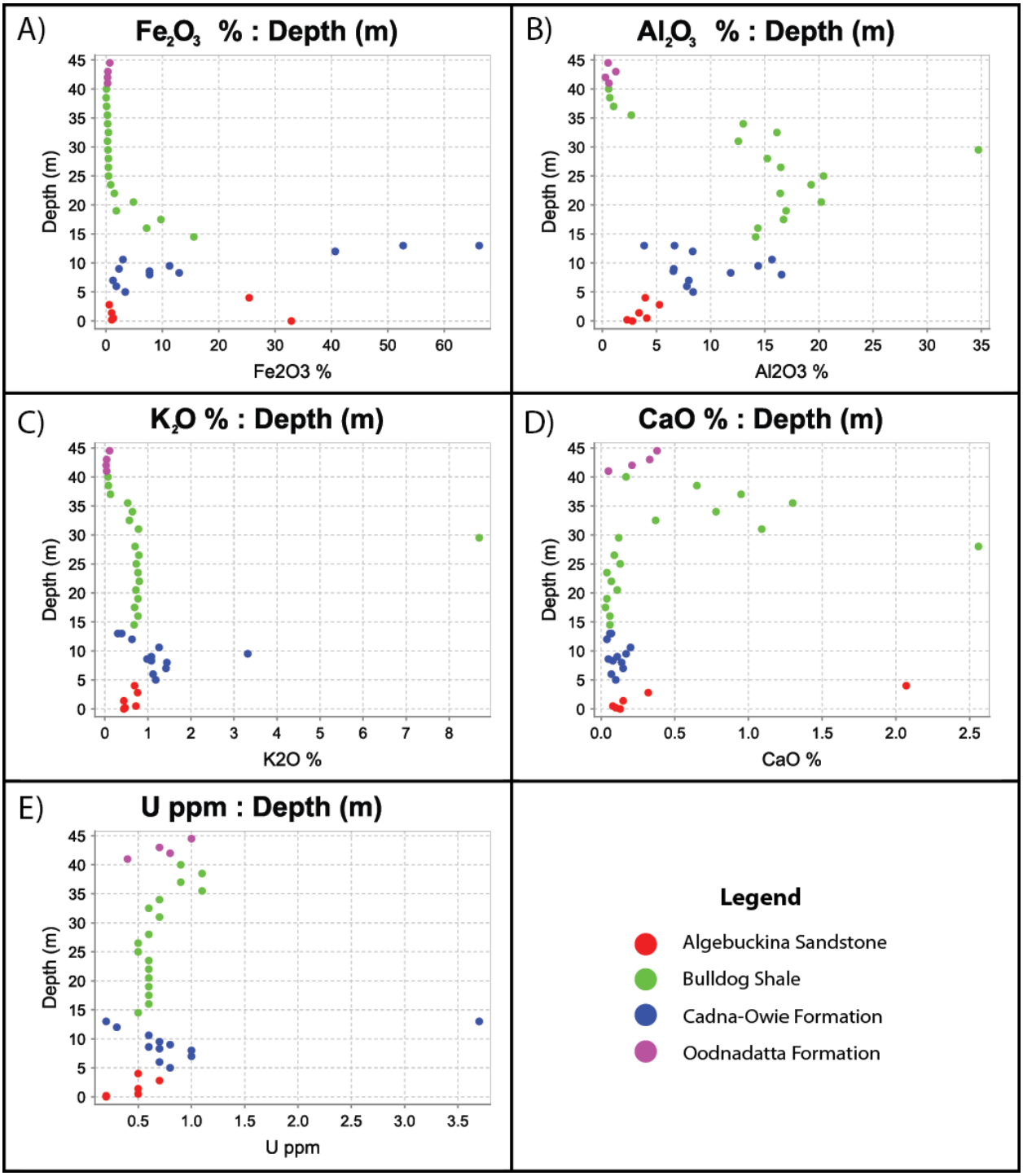

Figure 8: Down hole XY scatter plot of the Trinity Well type section with depth (m) with respect to a) Fe_2O_3, b) Al_2O_3, c) K_2O, d) CaO and e) U.

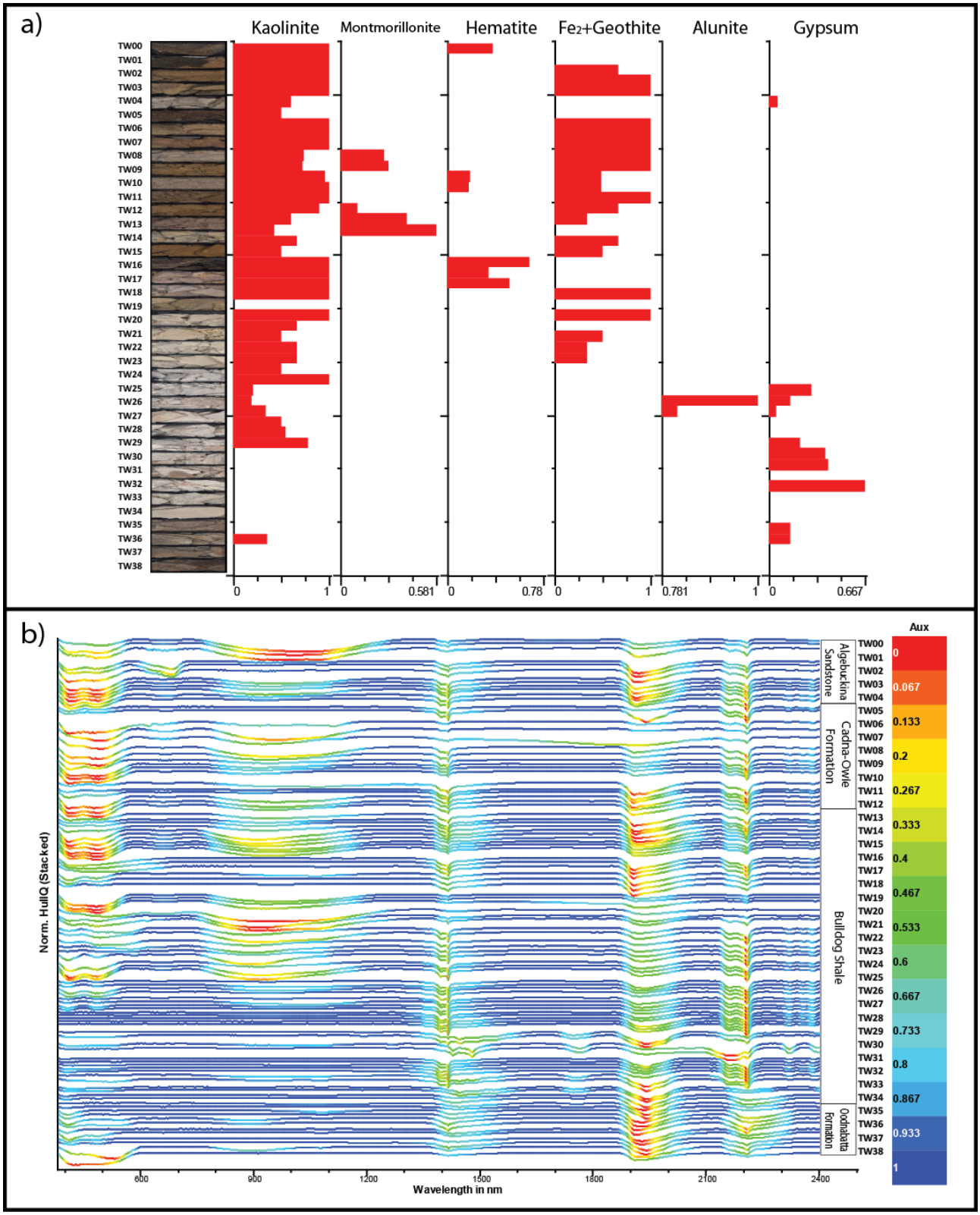

Figure 9: Trinity Well Type Section a) HyLogger down chip tray interoperation produced via CSRIO The Spectral Geologist 7.0 for the first of two passes showing relative amounts of various minerals with corresponding photo of the sample in the black chip tray. b) All spectral signatures stacked for the first of two passes with corresponding sample ID and stratigraphic unit labels for each signature.

4.3 Ludbrook Reference Section

The Ludbrook profile includes 12 sample points, consisting of a series of laterally offset profiles across a single, shallow dipping stratigraphic section. The stratigraphically higher profile was first sampled with samples labelled LUD01 through to LUD06. The lower profile was labelled LUD07 through to LUD12. The samples have been renamed LUDS01 through to LUDS12 to correspond with the stratigraphic order of the profiles. A combination of geochemical analysis and HyLogger core scanner data was acquired for the section, as well as sample LUDS10 (LUD04) selected for detrital zircon studies.

	Range	Minimum	Maximum	Mean	Std Dev.
SiO_2	71.50	24.20	95.70	63.08	17.60
Al_2O_3	18.56	0.75	19.31	13.09	6.68
Fe_2O_3	22.67	0.85	23.52	6.41	6.01
CaO	14.82	0.13	14.95	1.96	4.26
MgO	1.46	0.05	1.51	0.93	0.50
Na_2O	1.94	0.02	1.96	0.98	0.60
K_2O	2.21	0.26	2.47	1.76	0.85
MnO	0.60	0.01	0.61	0.09	0.17
TiO_2	0.88	0.08	0.96	0.67	0.33
TOT/C	0.21	0.09	0.82	0.33	0.25
TOT/S	0.15	0.04	0.44	0.19	0.13

Table 4: Summary statistics of major elements from the Ludbrook type section. n=12.

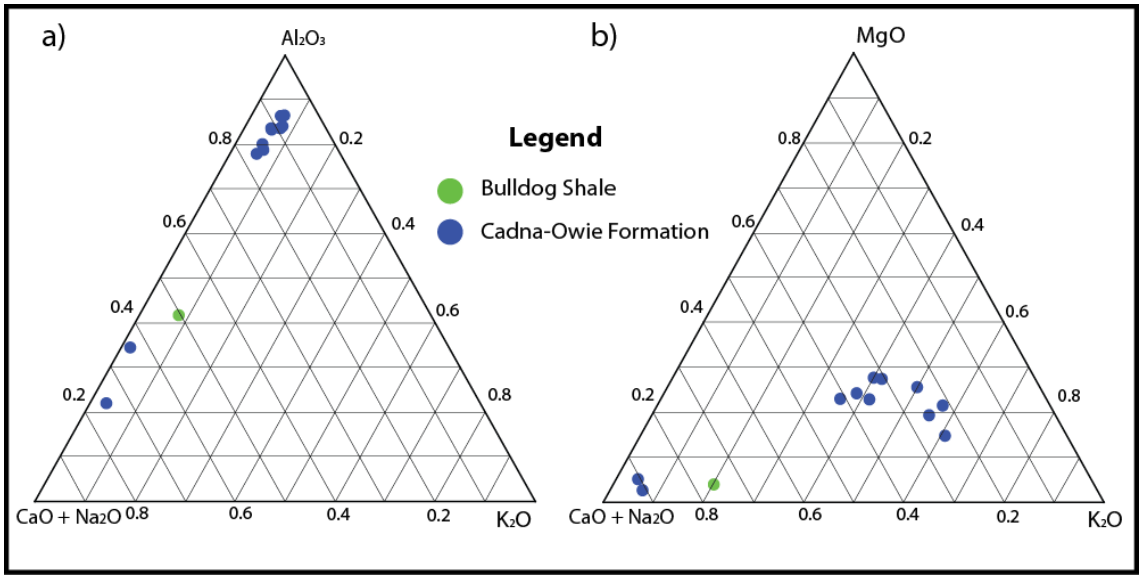

Figure 10: a) A-CN-K ternary plot for all Ludbrook samples, b) M-CA-K ternary plot for all Ludbrook samples.

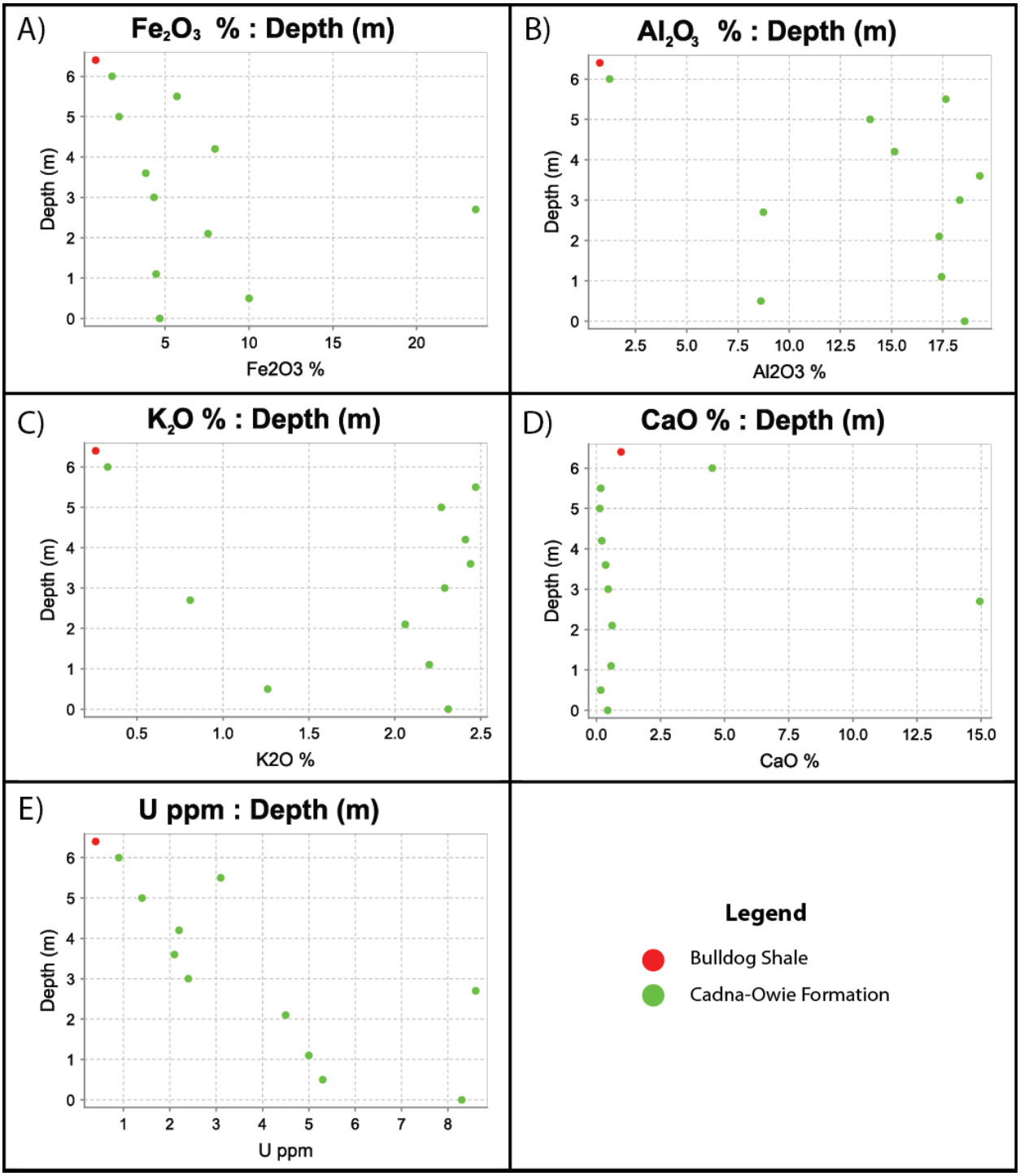

Figure 11: Down hole XY scatter plot of the Ludbrook type section with depth (m) with respect to a) Fe_2O_3, b) Al_2O_3, c) K_2O, d) CaO and e) U.

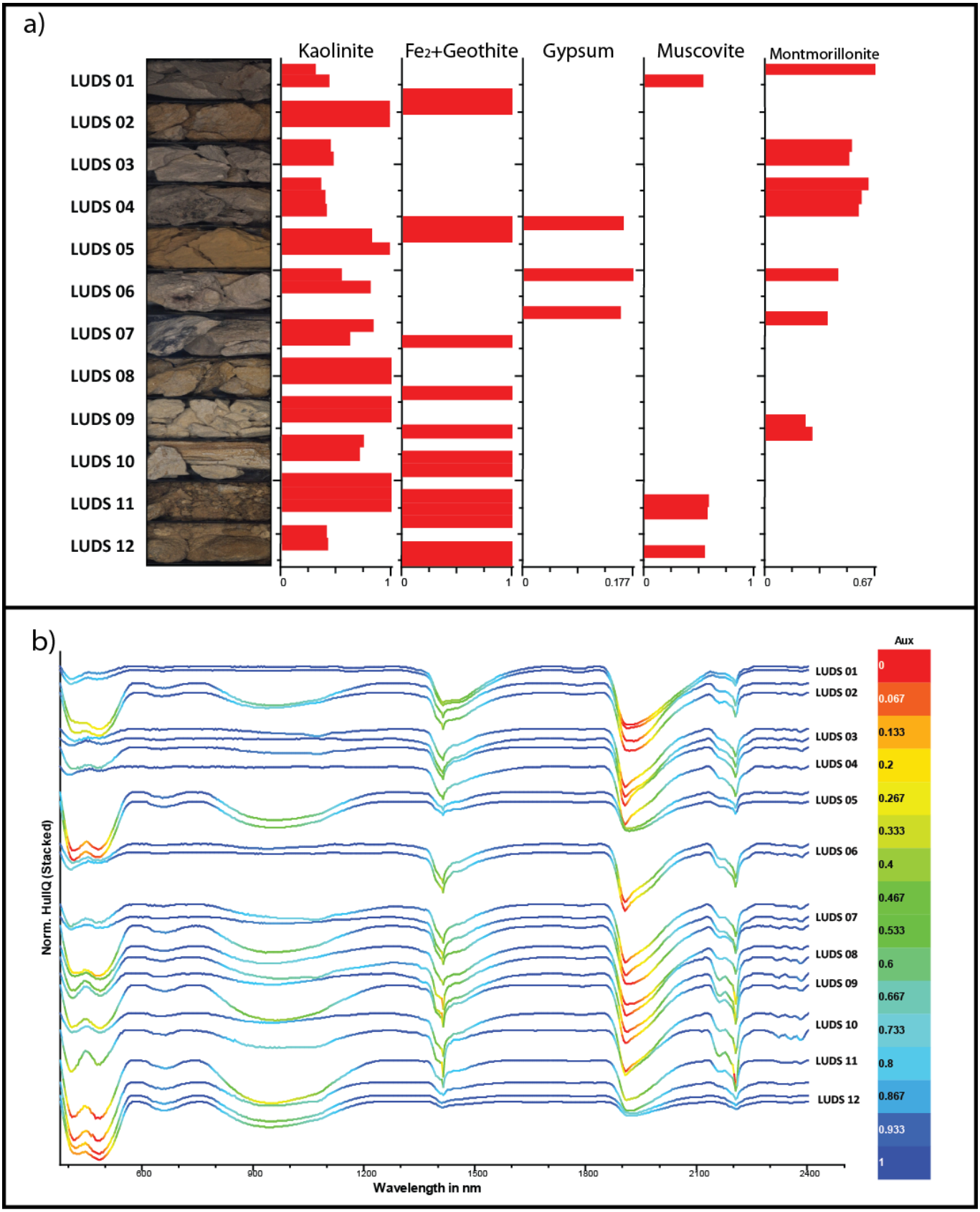

Figure 12: a) Ludbrook Reference section HyLogger down chip tray interoperation produced via CSRIO The Spectral Geologist 7.0 for the first of two passes showing relative amounts of various minerals with corresponding photo of the sample in the black chip tray. b) All spectral signatures stacked for the first of two passes with corresponding sample ID.

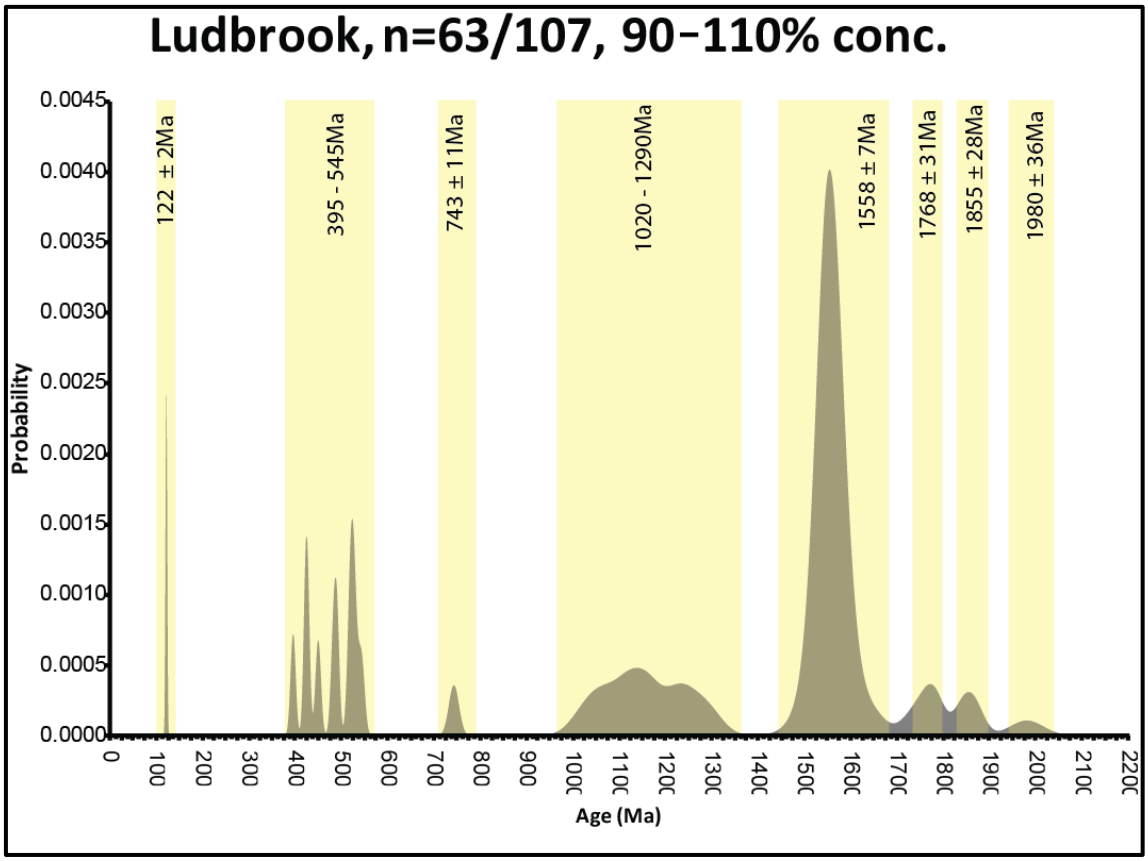

Figure 13: Probability density plot of all 63 within 10% concordant zircon analysis from 107 analysis conducted. Unique ages and age domains highlighted showing a wide spread of ages within sample LUD04.

5. DISCUSSION

5.1 Geochemistry

Geochemical trends and variations identified within the profiles and between the various type sections are difficult to quantify using basic statistical approaches. This is due to the variable nature of the sediments, where one or two samples can distort the results because of anomalously high or low values in one or more elements. Due care was taken when sample collecting as to not contaminate samples with adjacent sampling horizons.

5.1.1 Recorder Hill

The Recorder Hill type section includes 16 sample points from the Cadna-owie Formation, except for the uppermost sample that is from the base of the Bulldog Shale. The Cadna-owie Formation is composed of fine to medium grained feldspathic sandstones with silt and calcareous sandstone beds. For the major host elements there is a sharp and distinct change in the major element concentrations, in particular CaO where values change from 0.2% to 20% within two sample points, which are expressed as calcareous cemented units within the formation. High concentrations in trace elements La (44.8 ppm), Ce (97.9 ppm) and Nd (42.5 ppm) occur throughout the profile, which are in contrast to the low levels of Mo (1.5 ppm). The elevated levels of Al_2O_3, CaO, Na_2O and K_2O are attributed to feldspar minerals. These elements can be plotted in an A-CN-K ternary plot (Figure 3), which gives an indication of the degree of weathering feldspar to a kaolin secondary product (represented on the diagram by increasing Al_2O_3 levels). In Figure 3, the samples plot along a line showing decreasing levels of CaO and Na_2O with a marginal drop in concentration of K_2O. This suggests that many of the samples contain primary feldspars. There are two distinct groups plotted on the ternary diagram, the lower more CaO + Na2O dominate group representing the calcareous samples and the higher more weathered Al_2O_3 rich group representing the more clay rich samples. Samples RH01 and RH16 do not fit into either of the two major groups in the A-CN-K plot. This is interpreted to be due to sample RH01 being heavily influenced by the underlying weathered Adelaidean basement geology; and sample RH16 representing the lower section of the Bulldog Shale. When the geochemistry of the two major groups are examined in isolation rather than as a part of the entire data set from the profile, these samples show more consistent and less

variable results. This leads to recalculation of what is an anomalous or background value for the individual groups rather than as a whole for the entire data set. As sample RH07 was also selected for detrital zircon analysis, it was duplicated. The original RH07 sample collected three years prior plots in the lower more CaO + Na2O dominate group while the duplicate sample plots on the rim of the upper Al_2O_3 rich group. This is interpreted to be due to irregular oscillations in the calcareous cementation within the bed.

The Recorder Hill Type Section spans 17 meters vertically up. Figure 4a shows a very notable distinction between the Cadna- owie Formation and the Bulldog Shale, as the Cadna-owie Formation shows consistently low levels (1% - 5%) of Fe_2O_3 with a slight increase moving up the profile. The Bulldog Shale has a very sharp and distinct increase in Fe_2O_3 to 40%. This distinct change between units is not evident in the concentration of Al_2O_3, K_2O, CaO and U. Figure 4a, c and e show wide variations in levels of Al_2O_3, K_2O and U, but present similar distribution patterns respectively. Most notably at between depths 7.5 m and 12.5 m there is a cluster of high concentrations of these elements. Between 7.5 m and 12.5 m CaO displays near 0% levels (Figure 4d) as opposed to the high levels in Al_2O_3, K_2O and U.

5.1.2 Trinity Well

The Trinity Well Type Section at Western Spur includes the Algebuckina Sandstone, Cadna-owie Formation, Bulldog Shale and the Eyre Formation. A larger sample mass of TW16 was taken with the intention of obtaining detrital zircon grains but prior to mounting of the grains it was deemed unfeasible as not enough zircon grains were

extracted to produce a statistically viable data set. A portion of this sample was geochemically analysed as a duplicate sample giving a total of 40 samples.

The Algebuckina Sandstone is a kaolinite rich, predominately fine grained quartz sandstone with medium grained cross-bedding. Dominated by typically high SiO_2 (94.50%), moderate levels of Al_2O_3 (5.27%) and low levels of CaO (2.07%), MgO (0.22%), Na_2O (0.08%) and K_2O (0.76%), it also presents low levels of Fe_2O_3 (2%) with the exception of the upper most and lower most samples where there are lower levels of SiO_2 (57.30%) and higher levels of Fe_2O_3 (32.88%). This is interpreted to reflect leaching from the basement geology and the overlying Cadna-owie Formation. The Algebuckina Sandstone has been highly weathered and kaolinised, with Dart and Hill (2012) suggesting that this correlates to a low energy depositional environment and that the sediments are locally sourced. This is supported by the work of Pontual (2007), and from the low degree of crystallised kaolinite (HyLogger data presented below in section 5.3.1.).

The Cadna-owie Formation is also present at the Recorder Hill Type Section with a lithological description given previously. The Bulldog Shale is very fine grained carbonate- rich with high levels of Al_2O_3 (16.55%) but decreasing drastically towards the top of the profile (1.55%) as observed in Figure 8b. It has moderate SiO_2 (80%) concentrations and low amounts of Fe_2O_3 (5%) that decrease further up through the profile. This is an indication that this profile is susceptible to leaching of Fe_2O_3 from the underlying profile. Low levels of CaO (0.20%), MgO (0.04%), Na_2O (2%) and K_2O (3.2%) are evident through the profile with MnO levels below detection limits for most

of the profile. The Eyre Formation makes up only the upper most 4 samples and has been highly silicified to form a pedogenic silcrete that includes very high levels of SiO_2 (95%) in contrast to its very low levels of Al_2O_3 (1%), Fe_2O_3 (0.6%), CaO (0.35%), MgO (0.05%), Na_2O (0.03%) and K_2O (0.10). Geochemically, the Eyre Formation at Trinity Well is near to identical to the silicified top 3 layers of the Bulldog Shale that underlie the samples but visually the two are distinct. This causes problems when attempting to classify these formations based on their geochemistry alone.

The whole-rock geochemical results facilitate an assessment of the feasibility to geochemical distinguish stratigraphic units and lithologies, and potentially sub-divide these units further on the basis of their geochemistry. As a whole the Trinity Well type section is high in SiO_2 but with low levels of Al_2O_3. These two key features are emphasised when plotting ternary plots (Figure 7). The high degree of weathering over the whole profile has resulted in a large cluster of the sample points near Al_2O_3 (Figure 7a). If K_2O is replaced by $SiO_2/10$ (Figure 7b) the data falls into four clusters highlighted in red, blue, yellow and green. The Eyre Formation plots in a tight cluster towards the bottom right with near 100% SiO_2 (indicated with a green zone), this is attributed to the silification of the Eyre Formation from the Lake Eyre Basin. The Algebuckina Sandstone plots across a wider spread of compositions, trending towards higher concentrations of Al_2O_3 (indicated by the yellow zone). The Cadna-owie Formation plots into two distinct zones (the blue and red respectively). There is a large cluster of the Bulldog Shale samples that plot proximal to high to Al_2O_3 values, and 6 Cadna-owie samples that are also compositionally similar (red zone). These are the uppermost samples from the Cadna-owie Formation, immediately underlying the

Bulldog Shale. A similar trend occurs where the upper three samples from the Bulldog Shale plot within the green zone of the Eyre Formation. This is interpreted to represent a siliceous overprint throughout these samples. This trend is shown again in Figure 7c where Fe_2O_3 is substituted for $CaO + Na_2O$ resulting in a greater spread of the data. Samples from the green zone have not varied due to their high SiO_2 levels. The blue and yellow zones have now been spread across to Fe_2O_3, allowing for a clearer differentiation between the Cadna-owie Formation and the Algebuckina Sandstone.

Spanning a depth of over 45 m, Figure 8 gives down profile visualisation of various major and trace elements. Fe_2O_3 exhibits a variable range of concentrations below 20 m, ranging from 1% through to 67%; above 20 m Fe_2O_3 is consistently at or near 0% concentration (Figure 8a). The middle to upper Bulldog Shale and Eyre Formation make up the profile above 20 m. Al_2O_3 concentrations increases upwards through the profile and peaks at 25 m, before decreasing and levelling out at 35 m (Figure 8b). Both the Eyre Formation and Algebuckina Sandstone plot in small prominent clusters, but the Cadna-owie Formation and Bulldog Shale are not notably distinguishable based on Al_2O_3. K_2O is more resistant through the profile showing very little change in concentration (Figure 8c). Similar to Al_2O_3, both the Algebuckina Sandstone and Eyre Formation plot with a small spread comparable to the Bulldog Shale. Down-hole plots of CaO and U concentrations (Figure 8d & e respectively), indicate that the upper and lower sections of the profile have increased levels of these elements, whilst the middle of the profile is consistently low in concentrations. Similarities in the patterns between U and CaO support that CaO can be used as a pathfinder element for U in this instance.

5.1.3 Ludbrook

In the Ludbrook section the first 11 samples are from the Cadna-owie Formation while the uppermost sample is from the Bulldog Shale. Distinct sub- groups are evident when he data are plotted on a A-CN-K ternary diagram (Figure 10a). The more calcareous samples plot towards $CaO + Na_2O$, while the more clay-rich samples plot closer to pure Al_2O_3 origin. The Ludbrook profile is mostly dominated by clay-rich horizons. To help refine this group, MgO rather than Al_2O_3 is included in the ternary plot (Figure 10b). The calcareous zone then appears in the lower left sector towards $CaO + Na_2O$, but the clay zone is divided into two groups, further refining the geochemical signatures.

The Ludbrook section is the shortest of the three, with an overall depth of less than 10 m. It shows irregular geochemical variations through its profile. Similar to the Recorder Hill Type Section, it is mostly composed of Cadna-owie Formation with the uppermost sample being of the Bulldog Shale. The transition zone between these two units is masked with the uppermost sample of the Cadna-owie Formation presenting very similar characteristics to the Bulldog Shale. In Figure 11a, there is a weak trend towards a decrease in Fe_2O_3 when moving up through the profile. This is in contrast to U (Figure 11e), where there is a very clear decreasing trend of U moving up through the profile. Figure 11b and c show very similar signatures through the profile for Al_2O_3 and K_2O respectively, while Figure 11d shows CaO to have an overall very low presence throughout the depth of the profile. A key similarity between all the geochemical signatures is at a depth of 2.7 m, where this sample plots away from the bulk of samples in the profile.

5.2 Detrital Zircon Analysis

5.2.1 Recorder Hill Sample RH04

Sample RH04 had 98 zircon analyses. Due to a larger number of zircons containing high levels of common Pb there is a significantly reduced number of concordant zircon grains. Those grains that are within 10% concordancey total 44 displayed in (Figure 6). Nine direct ages and two age ranges have been extracted from the data set, the oldest of these being 2707 ± 21 Ma and 2011 ± 22 Ma. These are not a common age within previous studies but are potentially sourced from the Glenburgh Terrane within the Capricorn Orogeny (Neumann and Fraser 2007). The younger of these two ages is potentially the result of reworking within the Gawler Craton (Belousova *et al.* 2009). An 1839 ± 27 Ma peak may be sourced from the Mount Isa Inlier where the earliest major magmatic event is dated to 1840 Ma (Pell *et al.* 1997). Following on from this, a 1763 ± 22 Ma peak is also interoperated to have been derived from the Mount Isa Inlier (Page *et al.* 2000, Neumann and Fraser 2007); Specifically from zircons sourced from the Gunpowder Creek Formation and Paradise Creek Formation. Dominant peak events at 1654 ±31 Ma, 1558 ± 14 Ma and 1480 ± 27 Ma are interpreted to have been predominantly locally sourced from Mount Painter Inlier (Wülser *et al*. 2011) with minor influences from the Gawler Craton. Within the Gawler Craton they can be constrained to the Tarcoola Formation, deposited in the Wilgena Domain, the Nawa Domain and the Spilsby Suite respectively (Neumann and Fraser 2007, Payne *et al.* 2006). Three broad peaks are interperated to be derived from the Musgrave Block, ranging from 1380 Ma to 1023 Ma. Within the Musgrave Block the older zircons are sourced from the northern margin of the block, while the younger are sourced from the western margin (Pell *et al*. 1997). The next youngest age peaks are at 887 ± 11 Ma, 668

± 10 Ma, and a broad range of peaks at of 403-590 Ma age. These are mixed ages from sources such as the Lachlan Fold Belt, New England Fold Belt and the Adelaide Geosyncline (Pell *et al*. 1997, Swain *et al.* 2005, Wülser *et al.* 2011). The Delamerian Orogeny is interpreted to provide the most dominant source to the 403-590 Ma age range (Pell *et al*. 1997, Neumann and Fraser 2007).

5.2.2 Ludbrook Sample LUD04 (LUDS10)

LUD04 from the Ludbrook section had 107 zircon spots analysed with 63 of these falling within 10% concordia due to high levels of common Pb in the sample, similar to sample RH07. Figure 13 displays the six direct ages and two age ranges that have been extracted from the data. Many of these ages are also represented in the RH04 sample. The oldest age extracted in 1980 ± 36 Ma, believed to be derived from the Arunta Inlier (Pell *et al*. 1997). Peak events at 1855 ± 28 Ma and 1768 ± 31 Ma are interpreted to have been sourced from the Mount Isa Inlier, similar to the same peaks in RH04. A very dominant population is at 1558 ± 7 Ma that is also prevalent in sample RH04. The age domain 1290 Ma to 1023 Ma is interpreted to again represent the Musgrave Block. A 743 ± 11 Ma peak is likely to be sourced the eastern margin of the Adelaide Geosyncline (Pell *et al*. 1997). An age range of 543 Ma to 396 Ma, similar to the 590 Ma to 403 Ma peaks seen in RH04, believed to have been sourced from the Lachlan Fold Belt, New England Fold Belt and the Adelaide Geosyncline. Unlike the RH04 sample, a very sharp and dominant peak at 122 ± 2 Ma is likely to have been locally sourced from the Mount Painter Block where zircon and rutile ages have been found as young as 100 Ma (Pell *et al*. 1997, Wülser *et al*. 2011)

The detrital zircon spectra suggest that most of the sediments were sourced from a north-eastern direction. These are largely derived from north-eastern Queensland through to the Northern Territory across an arc shaped source region encompassing the Musgrave Block, whilst mostly showing a dominance of locally sourced sediments from the Mount Painter Inlier.

5.3 HyLogger

The stacking of the spectral signatures along the y-axis with respect to distance along the chip tray provides indications of kaolinite crystallinity through the profile and extrapolates the degree of transportation for the material. Transported and residual kaolinites are distinguished on their degree of crystallinity; whereby typically residual kaolinite grains are highly crystalline, and transported kaolinites are commonly poorly crystalline (Pontual 2007). This is indicated in the HyLogger data when the absorption becomes weaker and displays a shift from 2160 nm to longer wavelengths with decreasing crystallinity. Very poorly crystalline kaolinites display a weak absorption near 2180 nm.

5.3.1 Recorder Hill

HyLogger data produced from the Recorder Hill chip tray show a clear distinction between the Cadna-owie Formation and the overlying Bulldog Shale. The Cadna-owie Formation at the Recorder Hill Type Section is a kaolinite rich sequence whereas the overlying Bulldog Shale is kaolinite poor. This is further supported by the A-CN-K ternary plot in Figure 3 where sample RH16 does not plot with the Cadna-owie samples. In both passes of the HyLogger there is detection of trace amounts of gypsum in sample RH03, as well as various trace levels of muscovite in samples RH04 through to RH14.

When the data from the two passes of the HyLogger are merged muscovite is detected in those 10 samples, but on each single pass there are samples with below detectable amounts. This shows that muscovite is hetrogeneously distributed within the sediments. Figure 5a shows varying levels of hematite in all samples except RH09 and trace levels of carbonates, siderite in RH01 and RH05 along with ankerite in RH05. From the stacked spectral signatures presented in Figure 5b, there is a shift towards longer wavelengths at 2160 nm and then a drop in absorption at 2180 nm. This signature is mimicked on the second pass of the HyLogger presented in appendix 2. This characteristic shift in absorption gives indication that stratigraphically higher in the profile there is a decrease in the crystallinity of kaolinite. From the work of Pontual (2007) this decrease in crystallinity is correlated with the degree of transportation of the sediments. The lowest units show the most distant provenance, with transport distance decreasing up the profile.

5.3.2 Trinity Well

The Trinity Well Type Section at Western Spur presents a more complex HyLogger data set, with 4 formations that are all kaolinite dominated. Figure 9a shows that kaolinite is absent only in samples TW31 through to TW34, where these 4 samples correspond with the silicified top of the Bulldog Shale. Iron-rich minerals, such as hematite, Fe_2 + Goethite and Fe_3 + Goethite, dominate in samples TW00 through to TW24 but is absent above TW24. High levels of muscovite exist in samples TW31 and TW32, where no detectable levels of kaolinite are recorded. In the upper third section of the profile there is detection of gypsum. From the stacked spectral signature diagram shown in Figure 9b each formation can be identified from the degree of crystallinity of kaolinite. The lowest formation, the Algebuckina Sandstone shows an increase in

kaolinite crystallinity, and there is a small transition zone of low degree crystallinity when transitioning into the Cadna-owie Formation. The top of the Cadna-owie formation is marked by 5 flat signatures indicating low degree of crystallinity. The Bulldog Shale shows a generally high level of crystallinity while the overlying Eyre Formation includes low to very low degrees of crystallisation. This is interperated to be due to the more recent deposition of the Eyre Formation, hence not having enough time to fully crystallise.

5.3.3 Ludbrook

Kaolinite and Fe_2 + Goethite dominate the Ludbrook profile as shown in Figure 12a. There is an overall moderate to high level of kaolinite throughout the profile. Where there is a decrease in kaolinite levels there are increases in detectable levels of montmorillonite. Gypsum only occurs in the middle 3 layers of the profile, while high levels of muscovite only appear in the uppermost single layer. A small occurrence is also noted in an adjacent profile from the chip tray, but this is believed to be contamination due to having very low levels and only detected on a one of the two passes. The stacked spectral signature presented in Figure 12b shows a very low degree of kaolinite crystallinity, whereas stratigraphically upwards in the profile (ie down the stacked profiles as presented in Figure 12b), there is a slight increase in the degree of crystallinity. The lower degree of crystallinity of the profile possibly gives an indication that the profile is young (Pontual 2007, Summers *et al.* 2011). As for the Recorder Hill profile, the material making up the lowest unit has the most distant source and the source distance decreases upwards in the profile.

6. CONCLUSION

Being able to improve the workflow of the mineral exploration process by reducing time and money spent on a location, is an ongoing effort. In this study three methods are used with two that can be implemented on location at a drill hole by retrofitting current rigs to aid in this process. At exploration sites, HyLogger and geochemical analysis systems can be adapted to current drill rig systems, and along with visual logging by an onsite geologist we can streamline and make the exploration process more accurate and efficient. Geochemistry is an effective method of determining stratigraphic changes within a profile, and allows for the identification of stratigraphic units. By then using non standard statistical methods we are able to plot the data, and identify sub units within the stratigraphy. Hylogger signatures over the same samples are shown to define stratigraphic changes via mineralogical changes while giving implications to the degree of transportation of the sediments. These changes are not as what is seen in the geochemical data, but together these two methods along with visual logging are able to work together to give a more accurate indication to what is coming through a drill rig. Provenance detrital zircon studies are able to highlight sources for the sediments, HyLogger can aid in this by giving indications for the degree of transportation of the sediments. HyLogger and zircon data together suggest there where there is a higher degree of crystallisation, there is a younger maximum depositional age and vice versa. The use of geochemistry with the aid of a HyLogger and visual logging can further refine lithological units to aid in more efficiently targeting areas of mineralisation.

7. ACKNOWLEDGMENTS

Dr Katie Howard for being an amazing care taker of all the honours students, there is no way to thank Dr Howard for all the words of knowledge and guidance that she has given all the students with her open door policy.

I would like to acknowledge Dr Steven Hill for being my supervisor for this project. Always having an open door policy and being extremely efficient in the turnaround of material has been greatly appreciated. The amount of guidance and words of wisdom related to this project and more have been overwhelmingly appreciated.

Dr Robert Dart for being my secondary supervisor, always happy to read material, give feedback and answer all my questions on the spot.

Steven Hore from DIMITER for the large input towards the field work relating to this project. It has been greatly appreciated for the amount of in depth knowledge of the study area and the amount of time taken out of his schedule to participate in the field work.

All the staff at Adelaide Microscopy for the tireless work getting us trained on the various equipment used to acquire data.

Georgina Gordon (DMITRE) and DET CRC for swift use of the HyLogger Core Scanner and analysis of data.

8. REFERENCES

ALLEY N. F. 1987 Palynological dating and correlation of Late Jurassic and Early Cretaceous sediments around part of the southern margin of the Eromanga Basin, *Unpublished Report Department of Mines and Energy South Australia. RB,* vol. 87, no. 059.

ALLEY N. F. 1993 Palynological dating and correlation of Mesozoic rocks along the Neales River between the Peak and Denison Ranges and Lake Eyre North. South Australia: Department Of Mines And Energy.

ALLEY N. F. 1998 Cainozoic stratigraphy, palaeoenvironments and geological evolution of the Lake Eyre Basin, *Palaeogeography, Palaeoclimatology, Palaeoecology,* vol. 144, no. 3–4, pp. 239-263.

ALLEY N. F. & FRAKES L. A. 2003 First known Cretaceous glaciation: Livingston Tillite Member of the Cadna-owie Formation, South Australia, *Australian Journal of Earth Sciences,* vol. 50, no. 2, pp. 139-144.

ANAND R. 2005 Weathering history, landscape evolution and implications for exploration, *Regolith landscape evolution across Australia: A compilation of regolith landscape case studies with regolith landscape evolution models. CRC LEME Monograph*, pp. 2-40.

ANAND R. R. & ROBERTSON I. D. M. 2012 The role of mineralogy and geochemistry in forming anomalies on interfaces and in areas of deep basin cover: implications for exploration, *Geochemistry: Exploration, Environment, Analysis,* vol. 12, no. 1, pp. 45-66.

ARMIT R. J., BETTS P. G., SCHAEFER B. F. & AILLERES L. 2001 Constraints on long-lived Mesoproterozoic and Palaeozoic deformational events and crustal architecture in the northern Mount Painter Province, Australia, *Gondwana Research*, no. 0.

AUSTRALIA G. S. O. S. 1969 Mount Painter Province 1:125,000. In COATS R. P. ed. Geological atlas special series*.* Adelaide: The Department.

BELOUSOVA E. A., REID A. J., GRIFFIN W. L. & O'REILLY S. Y. 2009 Rejuvenation vs. recycling of Archean crust in the Gawler Craton, South Australia: Evidence from U–Pb and Hf isotopes in detrital zircon, *Lithos,* vol. 113, no. 3–4, pp. 570-582.

BUTT C. R. M., LINTERN M. J. & ANAND R. R. 2000 Evolution of regoliths and landscapes in deeply weathered terrain — implications for geochemical exploration, *Ore Geology Reviews,* vol. 16, no. 3–4, pp. 167-183.

CALLEN R. A., ALLEY D. R. & GREENWOOD D. R. 1995 Lake Eyre Basin. The Geology of South Australia: The Phanerozoic*.* Mines and Energy, South Australia, Geological Survey of South Australia.

COATS R. P. & BLISSETT A. H. 1971 Regional and economic geology of the Mount Painter Province*.* Dept. of Mines, Geological Survey of South Australia.

DART R. & HILL S. 2012 Geochemical classification of the basal Mesozoic cover of the south-western Eromanga Basin, South Australia. pp. 1-67. The University of Adelaide: Deep Exploration Technologies cooperative Research Centre.

DREXEL J. F., PREISS W. V. & PARKER A. J. 1995 Eromanga Basin. The Geology of South Australia: The Phanerozoic*.* pp. 101-126, bulletin 54 ed.: Mines and Energy, South Australia, Geological Survey of South Australia.

ELLIS G. K. 1976 Lake Namba, Evaluation of Previous Drilling and Resistivity Results. In ENERGY S. A. D. O. M. A. ed. pp. 42.

FLINT R. B., AMBROSE G. J. & CAMPBELL K. S. W. 1980 Fossiliferous Lower Devonian boulders in Cretaceous sediments of the Great Australian Basin, *Royal Society of South Australia* vol. 104, pp. 57-66.

FODEN J., ELBURG M. A., DOUGHERTY-PAGE J. & BURTT A. 2006 The timing and duration of the Delamerian Orogeny; correlation with the Ross Orogen and implications for Gondwana assembly, *Journal of Geology,* vol. 114, no. 2, pp. 189-210.

FORBES B. G. 1982 Margin of the Eromanga Basin, South Australia: a review, *Petroleum Exploration Society of Australia Australia., Geological Society of Australia Australia. Pages*.

GRAVESTOCK D. I., MOORE P. S. & PITT G. M. 1986 Contributions to the Geology and Hydrocarbon Potential of the Eromanga Basin*.* Geological Society of Australia.

GRAY D. J., WILDMAN J. E. & LONGMAN G. D. 1999 Selective and partial extraction analyses of transported overburden for gold exploration in the Yilgarn Craton, Western Australia, *Journal of Geochemical Exploration,* vol. 67, no. 1–3, pp. 51-66.

GRIFFIN W. L., POWELL W. J., PEARSON N. J. & O'REILLY S. Y. 2008 Appendix A2; GLITTER; data reduction software for laser ablation ICP-MS, *Short Course Series Mineralogical Association of Canada,* vol. 40, pp. 308-311.

HOWARD K. E., HAND M., BAROVICH K. M., REID A., WADE B. P. & BELOUSOVA E. A. 2009 Detrital zircon ages: Improving interpretation via Nd and Hf isotopic data, *Chemical Geology,* vol. 262, no. 3–4, pp. 277-292.

JACKSON S. E., PEARSON N. J., GRIFFIN W. L. & BELOUSOVA E. A. 2004 The application of laser ablation-inductively coupled plasma-mass spectrometry to in situ U–Pb zircon geochronology, *Chemical Geology,* vol. 211, no. 1–2, pp. 47-69.

KEELING J., MAUGER A. & HUNTINGTON J. 2004 Spectral core logger update - preliminary results from the Barnes gold prospect, *MESA Journal,* vol. 33, pp. 32-36.

KELLEY D. L., HALL G. E. M., CLOSS L. G., HAMILTON I. C. & MCEWEN R. M. 2003 The use of partial extraction geochemistry for copper exploration in northern Chile, *Geochemistry: Exploration, Environment, Analysis,* vol. 3, no. 1, pp. 85-104.

LUDBROOK N. H. 1966 Cretaceous biostratigraphy of the Great Artesian Basin in South Australia, *Bull. Geol. Surv. S. Aust,* vol. 40.

NEUMANN N. L. & FRASER G. L. 2007 Geochronological synthesis and time-space plots for Proterozoic Australia*.* Geoscience Australia.

PAGE R. W., JACKSON M. J. & KRASSAY A. A. 2000 Constraining sequence stratigraphy in north Australian basins: SHRIMP U–Pb zircon geochronology between Mt Isa and McArthur River*, *Australian Journal of Earth Sciences,* vol. 47, no. 3, pp. 431-459.

PAYNE J. L., BAROVICH K. M. & HAND M. 2006 Provenance of metasedimentary rocks in the northern Gawler Craton, Australia: Implications for Palaeoproterozoic reconstructions, *Precambrian Research,* vol. 148, no. 3–4, pp. 275-291.

PELL S. D., WILLIAMS I. S. & CHIVAS A. R. 1997 The use of protolith zircon-age fingerprints in determining the protosource areas for some Australian dune sands, *Sedimentary Geology,* vol. 109, no. 3–4, pp. 233-260.

PONTUAL S. 2007 Characterisation of regolith profiles by infrared spectroscopy. 5th Sprigg Symposium*.* Adelaide: Geologyical Society of Australia.

SKIRROW R. G. 2009 Uranium Ore-forming Systems of the Lake Frome Region, South Australia: Regional Spatial Controls and Exploration Criteria*.* Geoscience Australia.

SLÁMA J., KOŠLER J., CONDON D. J., CROWLEY J. L., GERDES A., HANCHAR J. M., HORSTWOOD M. S. A., MORRIS G. A., NASDALA L., NORBERG N., SCHALTEGGER U., SCHOENE B., TUBRETT M. N. & WHITEHOUSE M. J. 2008 Plešovice zircon — A new natural reference material for U–Pb and Hf isotopic microanalysis, *Chemical Geology,* vol. 249, no. 1–2, pp. 1-35.

SMEE B. W. 1998 A new theory to explain the formation of soil geochemical responses over deeply covered gold mineralization in arid environments, *Journal of Geochemical Exploration,* vol. 61, no. 1–3, pp. 149-172.

SUMMERS D., LEWIS M., OSTENDORF B. & CHITTLEBOROUGH D. 2011 Visible near-infrared reflectance spectroscopy as a predictive indicator of soil properties, *Ecological Indicators,* vol. 11, no. 1, pp. 123-131.

SWAIN G. M., HAND M., TEASDALE J., RUTHERFORD L. & CLARK C. 2005 Age constraints on terrane-scale shear zones in the Gawler Craton, southern Australia, *Precambrian Research,* vol. 139, no. 3, pp. 164-180.

TEALE G. S. 1993 Geology of the Mount Painter and Mount Babbage inliers. In DREXEL J. F., PREISS W. V. & PARKER A. J. eds. The Geology of South Australia: The Phanerozoic*.* pp. 149-156. bulletin 54 ed.: Mines and Energy, South Australia, Geological Survey of South Australia.

WÜLSER P.-A., BRUGGER J., FODEN J. & PFEIFER H.-R. 2011 The Sandstone-Hosted Beverley Uranium Deposit, Lake Frome Basin, South Australia: Mineralogy, Geochemistry, and a Time-Constrained Model for Its Genesis, *Economic Geology,* vol. 106, no. 5, pp. 835-867.

Appendix 1

	SiO_2	$Al2O_3$	Fe_2O_3	CaO	MgO	Na_2O	K_2O	MnO	TiO_2	P_2O_5	Cr_2O_3	Ba	LOI	SUM	TOT/C	TOT/S
Sample ID	%	%	%	%	%	%	%	%	%	%	%	%	%	%	%	%
LUDS 01	57.9	18.57	4.67	0.44	1.51	1.25	2.31	0.05	0.96	0.17	0.005	0.04	11.98	99.90	0.41	0.08
LUDS 02	70.6	8.62	10.00	0.17	0.69	0.90	1.26	0.02	0.41	0.10	0.003	0.02	6.84	99.59	0.13	0.08
LUDS 03	56.7	17.44	4.46	0.57	1.41	1.96	2.20	0.03	0.93	0.16	0.003	0.04	13.03	98.95	0.33	0.27
LUDS 04	55.9	17.33	7.55	0.61	1.42	1.04	2.06	0.03	0.93	0.26	0.003	0.03	11.92	99.08	0.43	0.25
LUDS 05	24.2	8.74	23.52	14.95	0.92	1.55	0.81	0.18	0.47	10.74	0.002	0.05	12.70	98.83	0.78	0.28
LUDS 06	57.3	18.33	4.33	0.46	1.44	1.76	2.29	0.02	0.95	0.13	0.005	0.04	12.52	99.62	0.15	0.33
LUDS 07	58.4	19.31	3.84	0.36	1.25	0.84	2.44	0.61	0.94	0.13	0.003	0.14	11.88	100.13	0.19	0.09
LUDS 08	62.0	15.15	7.97	0.21	0.84	0.89	2.41	0.02	0.71	0.13	0.006	0.05	9.63	100.00	0.16	0.04
LUDS 09	71.8	13.95	2.25	0.13	0.55	0.78	2.27	0.05	0.58	0.05	0.002	0.05	7.08	99.50	0.09	0.09
LUDS 10	60.6	17.65	5.70	0.17	0.93	0.76	2.47	0.07	0.96	0.11	0.017	0.06	9.90	99.43	0.21	0.15
LUDS 11	85.8	1.23	1.83	4.52	0.13	0.04	0.33	0.02	0.08	0.02	0.003	<0.01	5.00	99.00	0.82	0.44
LUDS 12	95.7	0.75	0.85	0.96	0.05	0.02	0.26	0.01	0.15	<0.01	<0.001	<0.01	0.94	99.68	0.21	<0.02
RH01	68.8	7.02	2.15	9.83	0.21	0.17	0.36	0.05	0.34	0.02		<0.01	10.5	99.42	2.12	<0.02
RH02	83.1	9.09	2	0.14	0.28	0.36	0.85	0.04	0.32	0.02		0.01	3.99	100.22	<0.02	0.08
RH03	84.2	5.55	1.38	1.51	0.26	0.25	1.04	0.02	0.51	0.02		0.02	4.68	99.4	0.08	0.63
RH04	91.8	3.91	0.95	0.06	0.19	0.11	1.07	0.02	0.48	0.02		0.02	1.1	99.7	0.02	<0.02
RH 04 Dup	92.2	3.65	0.98	0.10	0.16	0.08	0.83	0.02	0.43	0.02	0.009	0.02	1.33	99.81	0.07	<0.02
RH05	59.7	3.76	2.45	17.09	0.39	0.12	0.68	0.04	0.27	0.03		0.02	15.15	99.71	3.87	0.02
RH06	58.3	6.78	2.02	15.86	0.49	0.1	1.03	0.06	0.44	0.04		0.03	14.89	100.06	3.58	<0.02
RH07	71.9	12.18	3.09	0.31	0.89	1.95	2.81	0.06	0.76	0.08		0.05	6.01	100.13	0.14	0.14
RH 07 Dup	61.4	4.87	2.24	14.99	0.47	0.11	1.11	0.03	0.39	0.03	<0.001	0.02	13.81	99.44	3.75	0.05
RH08	70.2	13.48	3.01	0.26	0.96	1.92	3.14	0.03	0.86	0.1		0.05	6.22	100.21	0.1	0.17
RH09	66.9	12.94	4.54	0.18	1.32	2.34	3.09	0.04	0.77	0.1		0.05	7.5	99.74	0.11	0.33
RH10	64.7	13.13	4.62	0.25	1.38	3.15	3.07	0.04	0.76	0.12		0.05	8.42	99.71	0.14	0.38
RH11	64.4	13.67	4.79	0.21	1.4	2.56	3.18	0.03	0.77	0.12		0.06	8.18	99.35	0.16	0.32
RH12	41.7	8.07	5.06	21.41	1.02	0.28	1.47	0.13	0.44	0.14		0.04	20.61	100.32	4.9	0.1
RH13	42.7	6.52	3.08	23.32	0.78	0.12	1.26	0.08	0.42	0.08		0.03	21.41	99.77	5.32	<0.02
RH14	51.8	16.82	5.97	0.4	1.97	4.94	2.84	0.11	0.85	0.22		0.05	12.67	98.62	0.23	0.54
RH15	45.4	7.7	3.37	20.27	0.96	0.28	1.55	0.09	0.5	0.11		0.04	19.55	99.85	4.57	0.05
RH16	26.9	5.2	39.57	6.96	2.06	0.39	0.82	3.51	0.33	0.48		0.04	13.9	100.14	1.73	0.1
TW00	57.3	2.77	32.88	0.13	0.1	0.05	0.44	0.06	0.1	0.41		0.02	5.92	100.13		
TW01	94.5	2.28	1.03	0.1	0.14	0.05	0.47	0.02	0.16	0.03		<0.01	1.01	99.75		
TW02	91.2	4.1	1.32	0.08	0.13	0.04	0.72	0.03	0.37	0.03		0.01	1.71	99.73		
TW03	91.7	3.38	1.01	0.15	0.22	0.07	0.44	0.04	0.29	0.03		0.02	1.83	99.15		
TW04	89.5	5.27	0.58	0.32	0.07	0.03	0.76	0.02	0.49	0.01		0.02	2.27	99.32		
TW05	58.4	3.96	25.41	0.32	0.17	0.08	0.69	0.23	0.36	0.11		0.03	7.39	98.93		
TW06	82.2	8.38	3.42	0.1	0.13	0.06	1.18	0.02	0.52	0.05		0.03	3.17	99.23		
TW07	85.4	7.8	1.84	0.07	0.14	0.05	1.12	0.02	0.52	0.05		0.03	2.85	99.92		
TW08	84.5	7.98	1.25	0.15	0.19	0.06	1.42	0.02	0.66	0.03		0.03	2.99	99.28		
TW09	60.5	16.55	7.75	0.14	0.87	1.73	1.44	0.01	0.91	0.23		0.04	10.07	100.24		

	SiO_2	$Al2O_3$	Fe_2O_3	CaO	MgO	Na_2O	K_2O	MnO	TiO_2	P_2O_5	Cr_2O_3	Ba	LOI	SUM	TOT/C	TOT/S
Sample ID	%	%	%	%	%	%	%	%	%	%	%	%	%	%	%	%
TW10	81.5	6.59	2.31	0.11	0.57	1.24	1.08	0.01	0.44	0.07		0.02	5.59	99.59		
TW11	73	6.55	7.72	0.05	1.07	1.9	0.98	0.01	0.4	0.11		0.02	7.72	99.51		
TW12	58.3	11.85	13	0.08	1.36	2.21	1.08	<0.01	0.62	0.25		0.02	11.15	99.95		
TW13	49.6	14.39	11.28	0.17	0.76	1.14	3.32	0.02	0.69	0.27		0.04	17.06	98.74		
TW14	65.8	15.66	3.01	0.2	1.24	1.41	1.26	0.02	0.71	0.49		0.06	9.53	99.35		
TW15	39.4	8.34	40.68	0.04	0.43	0.66	0.63	0.04	0.38	0.53		0.03	9.21	100.35		
TW16	22.3	3.86	66.22	0.06	0.12	0.14	0.3	0.03	0.25	0.55		0.02	6	99.85		
TW 16 Dup	32.5	6.66	52.72	0.07	0.16	0.18	0.39	0.03	0.34	0.62	0.006	0.03	6.63	100.34	0.12	0.15
TW17	60.1	14.15	15.59	0.06	0.21	0.7	0.68	0.02	0.63	0.36		0.05	7.8	100.3		
TW18	66.3	14.36	7.21	0.06	0.41	1.55	0.77	0.02	0.67	0.19		0.04	8.2	99.73		
TW19	62.4	16.73	9.74	0.03	0.31	1.01	0.69	0.01	0.67	0.21		0.04	8.42	100.29		
TW20	69	16.97	1.84	0.04	0.44	1.52	0.77	<0.01	0.71	0.05		0.03	8.66	100.01		
TW21	62.2	20.22	4.87	0.11	0.26	1.04	0.72	0.01	0.7	0.17		0.04	9.65	100.04		
TW22	69.3	16.42	1.49	0.07	0.4	1.49	0.8	<0.01	0.71	0.06		0.02	8.38	99.14		
TW23	66.8	19.28	0.84	0.04	0.34	1.47	0.77	<0.01	0.73	0.03		0.01	9.18	99.47		
TW24	65.6	20.43	0.47	0.13	0.37	1.65	0.73	<0.01	0.7	0.02		0.02	9.93	100.04		
TW25	68	16.47	0.43	0.09	0.68	1.95	0.79	<0.01	0.72	0.02		0.02	10.07	99.22		
TW26	69.1	15.23	0.44	2.56	0.12	0.15	0.7	<0.01	0.68	0.02		0.03	8.63	97.67		
TW27	7.5	34.74	0.35	0.12	0.09	0.98	8.7	<0.01	0.05	0.1		0.04	40.46	93.12		
TW28	76.4	12.56	0.28	1.09	0.15	0.13	0.78	<0.01	0.85	0.05		0.03	6.61	98.91		
TW29	74.2	16.12	0.44	0.37	0.13	0.1	0.57	<0.01	0.81	0.03		0.02	6.7	99.47		
TW30	78.1	13.01	0.3	0.78	0.11	0.13	0.64	<0.01	0.88	0.02		0.02	6.01	100.05		
TW31	88.3	2.67	0.26	1.3	0.05	0.12	0.53	<0.01	1.08	0.15		0.05	3.71	98.23		
TW32	92.3	1.03	0.11	0.95	0.01	0.08	0.13	<0.01	1.17	0.12		0.04	2.51	98.48		
TW33	94.3	0.68	0.04	0.65	<0.01	0.07	0.08	<0.01	1.33	0.05		0.02	1.95	99.19		
TW34	95.9	0.58	0.09	0.17	0.01	0.1	0.07	<0.01	1.22	0.03		0.01	1.21	99.4		
TW35	98.2	0.6	0.29	0.05	<0.01	0.02	0.04	<0.01	0.5	<0.01		<0.01	0.59	100.27		
TW36	97	0.28	0.28	0.21	<0.01	0.02	0.03	<0.01	0.83	0.02		<0.01	0.74	99.44		
TW37	95.9	1.24	0.34	0.33	0.01	0.03	0.04	<0.01	0.73	0.03		<0.01	1.35	100.04		
TW38	94.7	0.52	0.68	0.38	0.05	0.02	0.11	0.01	0.79	0.04		0.05	1.15	98.52		

	Ag	As	Au	Ba	Be	Bi	Cd	Ce	Co	Cs	Cu	Dy	Er	Eu	Ga
Sample ID	PPM	PPM	PPB	PPM	PPM	PPM	PPM	PPM	PPM	PPM	PPM	PPM	PPM	PPM	PPM
LUDS 01	<0.1	1.9	0.6	351	3	0.1	0.2	66.1	11.1	6.0	33.8	4.29	2.52	1.51	21.1
LUDS 02	<0.1	9.8	1.1	227	5	<0.1	0.3	35.3	11.8	2.4	11.2	3.45	2.41	0.69	8.4
LUDS 03	<0.1	4.5	1.1	354	2	0.1	<0.1	59.5	21.4	6.1	31.7	5.01	3.13	1.32	17.2
LUDS 04	<0.1	8.1	3.1	325	3	0.1	<0.1	59.7	25.4	8.5	42.5	6.28	4.31	1.65	18.8
LUDS 05	<0.1	8.4	<0.5	354	7	<0.1	0.9	114.6	38.5	4.3	16.4	41.14	43.10	6.37	8.9
LUDS 06	<0.1	2.7	1.0	395	3	0.1	<0.1	55.3	7.1	4.3	21.0	4.57	2.70	1.25	20.3
LUDS 07	<0.1	2.8	1.7	1442	5	<0.1	0.1	66.1	76.8	6.5	20.7	4.62	2.96	1.36	21.0
LUDS 08	<0.1	7.8	1.0	434	4	<0.1	0.1	51.5	11.5	9.4	24.6	5.76	3.56	1.52	16.4
LUDS 09	<0.1	3.1	1.1	505	1	<0.1	<0.1	44.3	13.2	3.8	13.5	3.68	2.20	1.02	12.2
LUDS 10	0.2	18.8	0.9	576	3	0.1	<0.1	69.4	49.9	2.9	34.5	5.77	3.29	1.65	20.0
LUDS 11	<0.1	11.3	5.2	81	2	<0.1	0.2	13.2	3.2	16.8	10.6	1.26	0.79	0.18	2.1
LUDS 12	<0.1	3.6	2.2	71	<1	<0.1	<0.1	10.8	1.1	0.4	5.4	0.98	0.53	0.11	1.2
RH01	<0.1	1.3	<0.5	62	<1	0.2	<0.1	39.4	3	0.8	5.1	4.21	2.59	0.85	7
RH02	<0.1	1.6	<0.5	104	1	0.2	<0.1	57	16.3	1.1	9.8	4.1	2.4	0.91	8.6
RH03	<0.1	1.2	1	210	<1	0.2	<0.1	50.4	6.6	3.5	8.7	3.38	2.11	0.59	7.6
RH04	<0.1	2	1.7	218	<1	<0.1	<0.1	78	4.2	1.2	5.4	4.26	2.65	0.66	5.2
RH 04 Dup	<0.1	1.2	0.8	153	1	<0.1	<0.1	49.1	4.3	1.1	6.5	3.07	2.10	0.52	4.4
RH05	<0.1	30.1	1	248	<1	<0.1	0.7	37.8	6.7	1.3	12.1	3.21	1.84	0.68	4.6
RH06	<0.1	4.3	<0.5	302	1	0.2	0.7	57.6	4.7	2.5	14.9	4.96	3.13	0.98	8.6
RH07	<0.1	4.3	1.2	483	2	0.3	<0.1	86.7	18.2	5.4	22.7	6.12	3.77	1.25	15.7
RH 07 Dup	<0.1	3.7	<0.5	248	<1	<0.1	0.2	44.3	7.3	1.5	8.2	3.52	2.14	0.55	5.2
RH08	<0.1	4	<0.5	526	2	0.4	<0.1	97.9	20.1	5.4	29	6.22	3.81	1.37	17.3
RH09	<0.1	3.8	0.6	519	2	0.3	0.2	88.1	15.6	5.5	26	6.36	3.85	1.33	16.6
RH10	<0.1	3.8	1	483	2	0.3	<0.1	85	18.1	5.4	30.4	6.16	3.69	1.32	16.4
RH11	<0.1	3.6	<0.5	463	2	0.3	0.1	82.8	17.2	5.2	31.1	5.97	3.5	1.31	16.6
RH12	<0.1	6.4	<0.5	334	1	0.1	0.5	65.9	9.9	3.1	15.3	5.9	3.43	1.28	9.1
RH13	<0.1	2.3	<0.5	354	<1	0.1	0.2	52.5	4.8	2	8.7	4.64	2.88	0.9	7.5
RH14	<0.1	2	<0.5	445	2	0.3	0.2	77.4	16.3	5.3	44.4	5.64	3.37	1.42	21.3
RH15	<0.1	2.8	1.1	373	1	0.1	0.6	52.8	6.6	2.9	10.8	3.82	2.44	0.79	8.7
RH16	<0.1	9.4	<0.5	332	2	0.2	0.2	31.7	9.5	3	11.7	3.56	2.34	0.64	9.4
TW00				0.1	0.04			68.1	144	23		11.68	13.13	14.3	57.8
TW01				0.07	<0.02			10.5	123	<1		1.58	1.84	6.6	5.1
TW02				0.1	<0.02			14.5	150	<1		2.04	2.3	10.3	3.1
TW03				0.11	<0.02			8.1	178	<1		1.34	1.4	7.5	3.3
TW04				0.05	0.15			10.2	168	<1		1.67	1.75	10.4	1.5
TW05				0.1	1.05			18.7	183	2		2.82	2.84	14.6	57.6
TW06				0.13	<0.02			12.6	258	1		1.98	2.13	12.1	4.3
TW07				0.13	<0.02			12.1	262	<1		1.99	2.14	12.5	1.8
TW08				0.18	0.02			25	272	<1		4.09	4.19	26.3	1.4
TW09				0.31	0.34			18.7	305	2		4.67	3.74	46.1	2.5
TW10				0.09	0.58			15.2	197	<1		2.94	2.72	26.8	1.1
TW11				0.06	0.65			11.7	168	<1		2.13	2.08	16.5	1.4
TW12				0.07	0.53			13.1	210	2		2.44	2.32	18.9	3.2
TW13				0.18	3.02			14.8	383	1		3.69	3.1	26.5	4

	Ag	As	Au	Ba	Be	Bi	Cd	Ce	Co	Cs	Cu	Dy	Er	Eu	Ga
Sample ID	PPM	PPM	PPB	PPM	PPM	PPM	PPM	PPM	PPM	PPM	PPM	PPM	PPM	PPM	PPM
TW14				0.1	0.25			35.1	326	2		19.3	9.67	186	8.6
TW15				0.09	0.12			37.8	180	8		6.8	6.91	27.7	20.9
TW16				0.14	0.1			18.5	215	4		4.91	5	9.9	11.4
TW 16 Dup	<0.1	35	<0.5	324	9	0.1	<0.1	18.4	11.6	4.2	56.9	4.64	2.55	1.08	9.6
TW17				0.04	0.1			13.2	448	3		2.68	2.94	10	7.1
TW18				0.03	0.15			10.8	332	2		1.99	2.12	10.2	3
TW19				0.03	0.09			11	453	2		1.99	2.22	9.5	4.1
TW20				0.03	0.09			9.8	286	<1		1.36	1.6	8.3	1.6
TW21				0.03	0.18			10.6	329	2		2.84	2.14	22.9	3.4
TW22				0.03	0.11			9.8	220	<1		1.55	1.65	11.1	1.1
TW23				<0.02	0.09			9.9	179	1		1.29	1.61	8.4	1.2
TW24				0.03	0.11			9.3	174	<1		1.19	1.52	8.2	0.6
TW25				0.05	0.17			9	182	<1		1.12	1.45	7.5	0.6
TW26				0.03	1.35			9.2	217	<1		1.12	1.41	8.3	0.7
TW27				0.18	12.93			2.3	333	1		0.81	0.63	7	1.4
TW28				0.04	0.52			10.6	273	<1		1.4	1.61	13.2	0.6
TW29				0.03	0.11			9	168	<1		1.14	1.46	9.7	0.4
TW30				0.03	0.27			9	190	<1		1.09	1.45	9.7	0.4
TW31				0.04	0.63			13.4	454	<1		3.78	2.99	46.5	0.4
TW32				0.03	0.39			12	366	<1		2.21	2.14	25.9	0.4
TW33				0.02	0.26			10.5	230	<1		1.43	1.81	13.3	1.2
TW34				<0.02	0.06			8.2	181	<1		0.85	1.2	6.8	0.3
TW35				<0.02	<0.02			3.9	106	<1		0.35	0.57	1.9	0.2
TW36				<0.02	0.08			7.7	130	<1		0.45	0.96	1.5	0.3
TW37				0.04	0.12			6.8	114	<1		0.45	0.99	1.3	0.8
TW38				0.11	0.13			6.8	546	<1		0.57	0.87	2.5	1.4

	Gd	Hf	Hg	Ho	La	Lu	Mo	Nb	Nd	Ni	Pb	Pr	Rb	Sb	Se
Sample ID	PPM	PPM	PPB	PPM	PPM	PPM	PPM	PPM	PPM	PPM	PPM	PPM	PPM	PPM	PPM
LUDS 01	5.06	4.7	0.16	0.95	28.7	0.39	0.3	9.1	27.7	11.8	9.1	7.30	66.7	<0.1	<0.5
LUDS 02	2.97	4.9	0.04	0.81	16.4	0.37	2.0	5.3	14.6	22.2	9.0	3.73	34.2	<0.1	<0.5
LUDS 03	4.70	5.9	0.02	1.13	27.9	0.47	0.2	10.7	26.9	13.8	11.4	6.60	68.6	<0.1	0.7
LUDS 04	6.27	4.9	0.04	1.41	29.5	0.64	0.4	10.0	29.8	19.8	11.1	7.11	66.6	<0.1	2.1
LUDS 05	32.54	2.6	0.26	13.48	81.4	5.96	5.1	5.0	63.0	47.0	7.1	12.53	30.6	0.1	2.2
LUDS 06	4.49	6.0	0.02	0.94	26.2	0.45	<0.1	10.7	24.1	10.4	7.9	6.36	63.2	<0.1	<0.5
LUDS 07	5.09	6.0	0.05	1.01	28.6	0.47	1.5	10.8	25.5	25.2	17.1	6.84	62.7	<0.1	<0.5
LUDS 08	5.86	5.9	0.07	1.25	24.9	0.55	0.7	10.0	25.0	19.6	11.5	6.14	62.3	<0.1	<0.5
LUDS 09	3.80	6.8	0.03	0.83	21.7	0.32	0.2	8.2	20.3	8.4	10.1	5.02	51.6	<0.1	<0.5
LUDS 10	6.58	9.9	0.25	1.25	28.7	0.52	0.5	12.5	26.6	30.6	21.0	7.09	60.4	<0.1	<0.5
LUDS 11	1.07	1.6	0.02	0.25	5.6	0.12	0.4	1.6	4.1	6.5	4.0	1.12	11.7	0.1	<0.5
LUDS 12	0.76	1.4	0.01	0.22	5.7	0.10	0.1	2.2	5.1	2.6	2.2	1.06	9.0	<0.1	<0.5
RH01	4.37	6.8	<0.01	0.88	21.9	0.39	<0.1	6.6	22.7	3.6	10.4	5.44	25.5	<0.1	<0.5
RH02	4.56	6	<0.01	0.8	26.7	0.35	0.2	6.5	29.5	10	5.8	7	44.8	<0.1	<0.5
RH03	3.33	9.1	<0.01	0.67	24.2	0.32	1.1	10.4	21.6	5.9	5.8	5.58	46.3	0.1	<0.5
RH04	4.67	15.6	<0.01	0.85	36.2	0.42	0.2	11.6	32.5	3.8	5.5	8.43	40	<0.1	<0.5
RH 04 Dup	3.04	9.8	<0.01	0.67	24.2	0.34	0.2	8.2	18.2	5.0	5.8	5.34	28.4	<0.1	<0.5
RH05	3.48	4.9	<0.01	0.63	19	0.26	1.5	5.7	18.2	5.9	5.7	4.55	45.8	0.9	<0.5
RH06	5.05	9.3	<0.01	1.06	29.3	0.47	0.4	9.7	28.5	5.8	6.9	6.9	66.7	<0.1	0.6
RH07	6.27	10.8	<0.01	1.26	41	0.59	0.5	16.5	39.5	11.8	10.5	9.86	118.2	<0.1	<0.5
RH 07 Dup	3.18	9.3	<0.01	0.78	22.9	0.38	0.3	8.7	17.9	5.0	5.3	5.09	47.4	<0.1	<0.5
RH08	6.73	12.3	<0.01	1.27	44.8	0.58	0.5	17.7	42.5	11.7	10.2	10.81	125.2	<0.1	<0.5
RH09	6.67	11.1	<0.01	1.28	41.8	0.57	0.9	15.8	40.8	12.9	13.2	10.14	115.4	0.1	0.6
RH10	6.51	10.2	<0.01	1.22	40	0.57	0.9	14.4	39.3	12.8	11.8	9.67	111	0.1	0.6
RH11	6.39	9.3	<0.01	1.16	37.9	0.53	0.7	13.8	38.1	11.8	11.5	9.28	109.6	0.1	0.7
RH12	6.1	4.4	0.01	1.18	30.1	0.46	0.4	8.2	29.3	8.8	8.4	7.07	70.9	0.1	<0.5
RH13	4.72	6.3	<0.01	1.01	23.4	0.41	0.1	8.3	23.2	4.5	6.4	5.77	57.9	<0.1	<0.5
RH14	6.04	6.2	0.01	1.15	32.3	0.51	0.5	12.4	34.3	13.8	15.1	8.25	87.9	<0.1	1.5
RH15	3.92	8	<0.01	0.81	25	0.38	0.2	8.9	23.8	6.2	5.6	5.68	68.2	<0.1	0.6
RH16	3.27	2.6	0.02	0.76	14	0.36	1.2	5	15	16.2	12.9	3.51	42.5	0.2	0.7
TW00	6.29	0.5		2.14	50.8	1.05		2.1	18.4			7.4	1.5		
TW01	1.45	0.9		0.29	45.8	0.15		2.6	16.9			8.2	1.4		
TW02	2.11	1.6		0.37	146.7	0.22		4.5	25.8			13.6	4.6		
TW03	1.41	1.2		0.23	103.8	0.13		3.8	18.8			10.2	3		
TW04	1.89	1.4		0.28	207.6	0.17		5.1	25.2			13.7	5.9		
TW05	2.8	1		0.47	247	0.26		4.8	34.6			18.5	6.4		
TW06	2.15	2.7		0.34	225.9	0.21		8.5	28.7			15.7	6.5		
TW07	2.22	4.7		0.34	285.3	0.21		7.6	30.2			16.6	7.9		
TW08	4.5	2.9		0.69	560.2	0.42		9.4	68.6			36.7	15.3		
TW09	7.28	5		0.69	267.9	0.34		18.6	89.7			42	7.4		
TW10	4.04	2.3		0.46	336.8	0.26		7.9	63.7			29.8	9.1		
TW11	2.65	2.3		0.36	260.5	0.21		8.9	38.7			20.2	7		
TW12	3.06	3.7		0.39	249.6	0.24		14.2	42			22.5	7.1		
TW13	5.29	4.1		0.55	210.5	0.27		20.6	61			35.2	6		

	Gd	Hf	Hg	Ho	La	Lu	Mo	Nb	Nd	Ni	Pb	Pr	Rb	Sb	Se
Sample ID	PPM	PPM	PPB	PPM	PPM	PPM	PPM	PPM	PPM	PPM	PPM	PPM	PPM	PPM	PPM
TW14	28.44	6.1		2.16	133.3	0.45		17.5	363			146	4.1		
TW15	5.34	13.4		1.14	77.9	0.58		10	71.4			30.6	2		
TW16	3.54	3.3		0.87	50.7	0.38		7.5	14.7			7.4	1.4		
TW 16 Dup	4.55	1.9	<0.01	0.94	9.3	0.4	3.2	3.6	11	34.3	32.1	2.32	20.2	0.2	2.9
TW17	2.24	3.9		0.5	128.4	0.27		19.5	24.7			14.2	3.7		
TW18	1.89	3.1		0.36	118.1	0.22		15.1	24.6			14.3	3.5		
TW19	2.02	3.1		0.37	124.4	0.21		16.1	23.7			13.9	3.8		
TW20	1.47	3.2		0.26	124.9	0.2		14.5	21.1			13.1	3.9		
TW21	4.82	3		0.39	130.1	0.2		18.1	52.3			29.8	3.7		
TW22	2.14	3		0.27	127.7	0.2		17.2	24.7			14.4	3.7		
TW23	1.47	2.7		0.24	137.1	0.21		17.2	20			12.3	4.2		
TW24	1.29	2.3		0.22	126.7	0.18		15.6	21.4			13.3	3.7		
TW25	1.25	1.8		0.21	125.1	0.19		15	20.2			12.2	3.8		
TW26	1.26	2.2		0.22	118.8	0.19		14.1	22.5			13.8	3.2		
TW27	1.01	<0.1		0.12	12.8	0.04		4.4	23.1			11.6	0.2		
TW28	1.83	2		0.25	141.9	0.2		12.5	35.9			20.5	3.4		
TW29	1.39	1.7		0.21	130.1	0.18		16.9	30			16.3	3.2		
TW30	1.33	2.3		0.2	140.9	0.19		19	25.2			15.6	3.7		
TW31	6.2	1.1		0.56	165.7	0.27		17.2	116			55.7	4.2		
TW32	3.3	0.3		0.36	170	0.24		16.1	91.5			52.2	4.1		
TW33	1.81	0.2		0.27	149.2	0.21		4.4	39.6			24.2	3.4		
TW34	1.03	0.1		0.18	186.5	0.17		3.9	19.6			12.3	4.7		
TW35	0.34	0.2		0.08	196.7	0.1		1.6	6			3.2	4.8		
TW36	0.35	<0.1		0.12	597.5	0.18		1.5	4.2			2.1	15.1		
TW37	0.3	0.1		0.12	555.6	0.18		1.9	4			2	14.7		
TW38	0.47	0.1		0.13	605.7	0.16		0.6	6			3.8	15.6		

Appendix 2

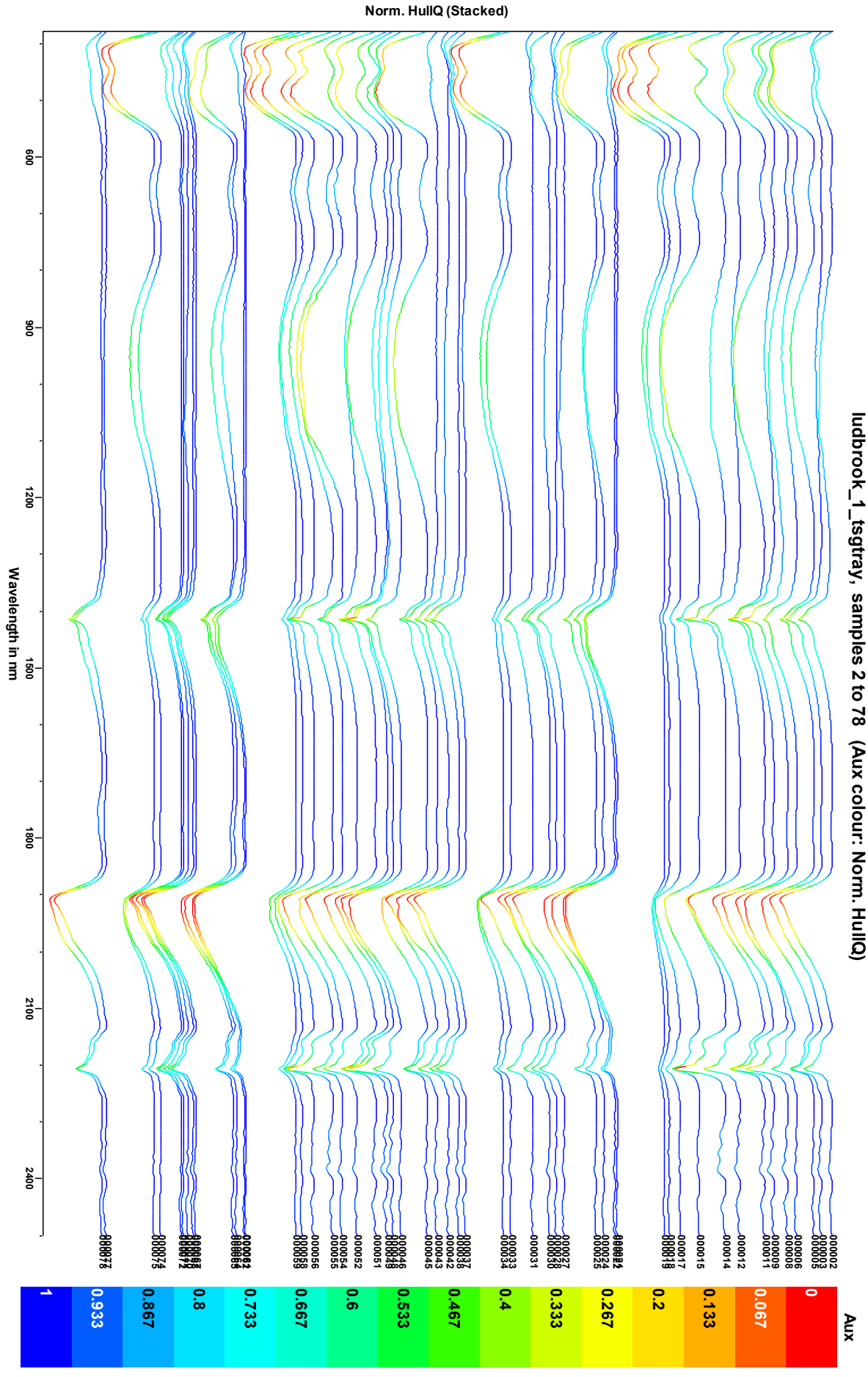
Norm. HullQ (Stacked)
ludbrook_1_tsgtray, samples 2 to 78 (Aux colour: Norm. HullQ)
Wavelength in nm
600
900
1200
1500
1800
2100
2400
Aux
0
0.067
0.133
0.2
0.267
0.333
0.4
0.467
0.533
0.6
0.667
0.733
0.8
0.867
0.933
1

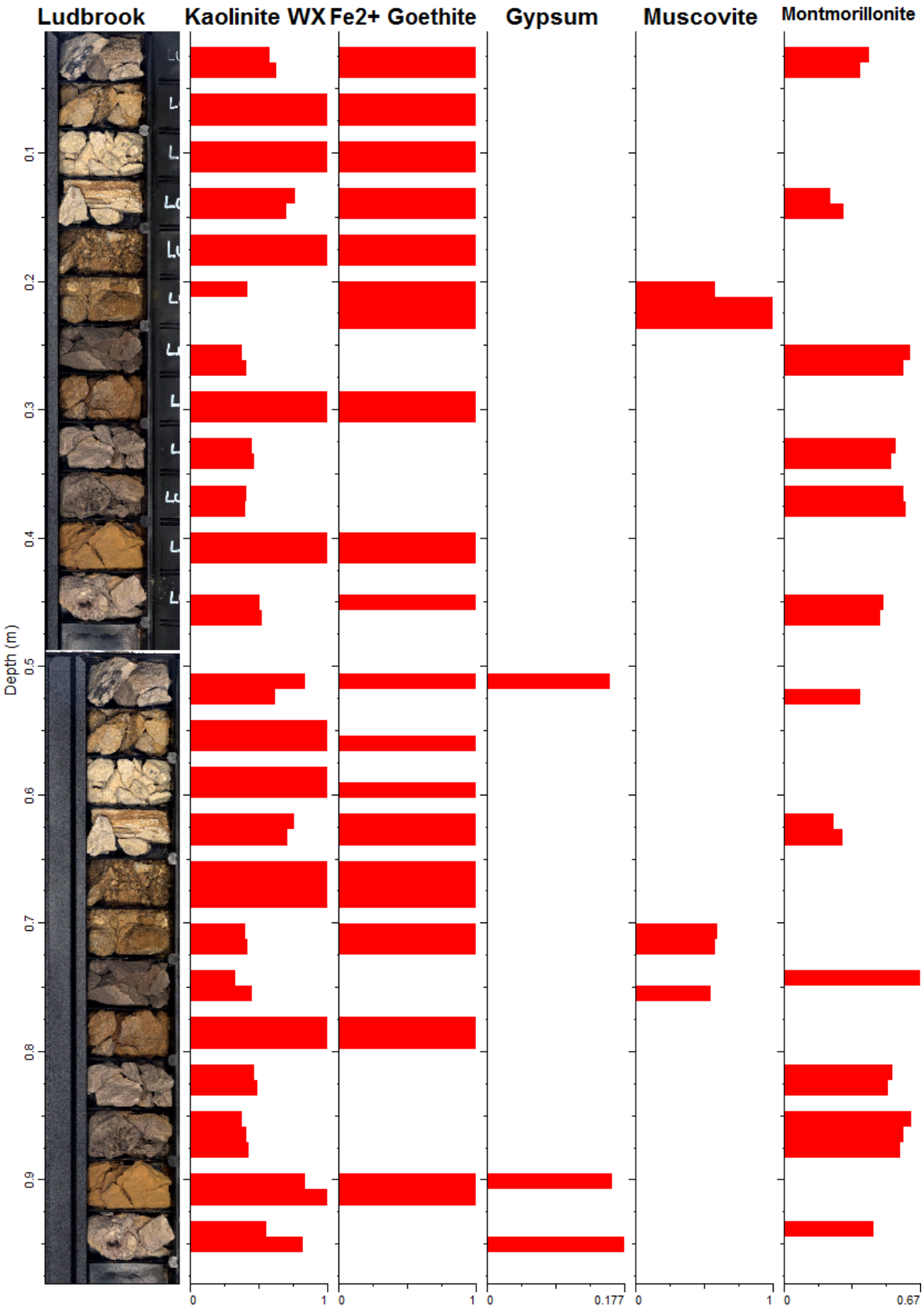
Ludbrook
Kaolinite WX
Fe2+ Goethite
Gypsum
Muscovite
Montmorillonite
Depth (m)
0.1
0.2
0.3
0.4
0.5
0.6
0.7
0.8
0.9
0
1
0
1
0
0.177
0
1
0
0.67

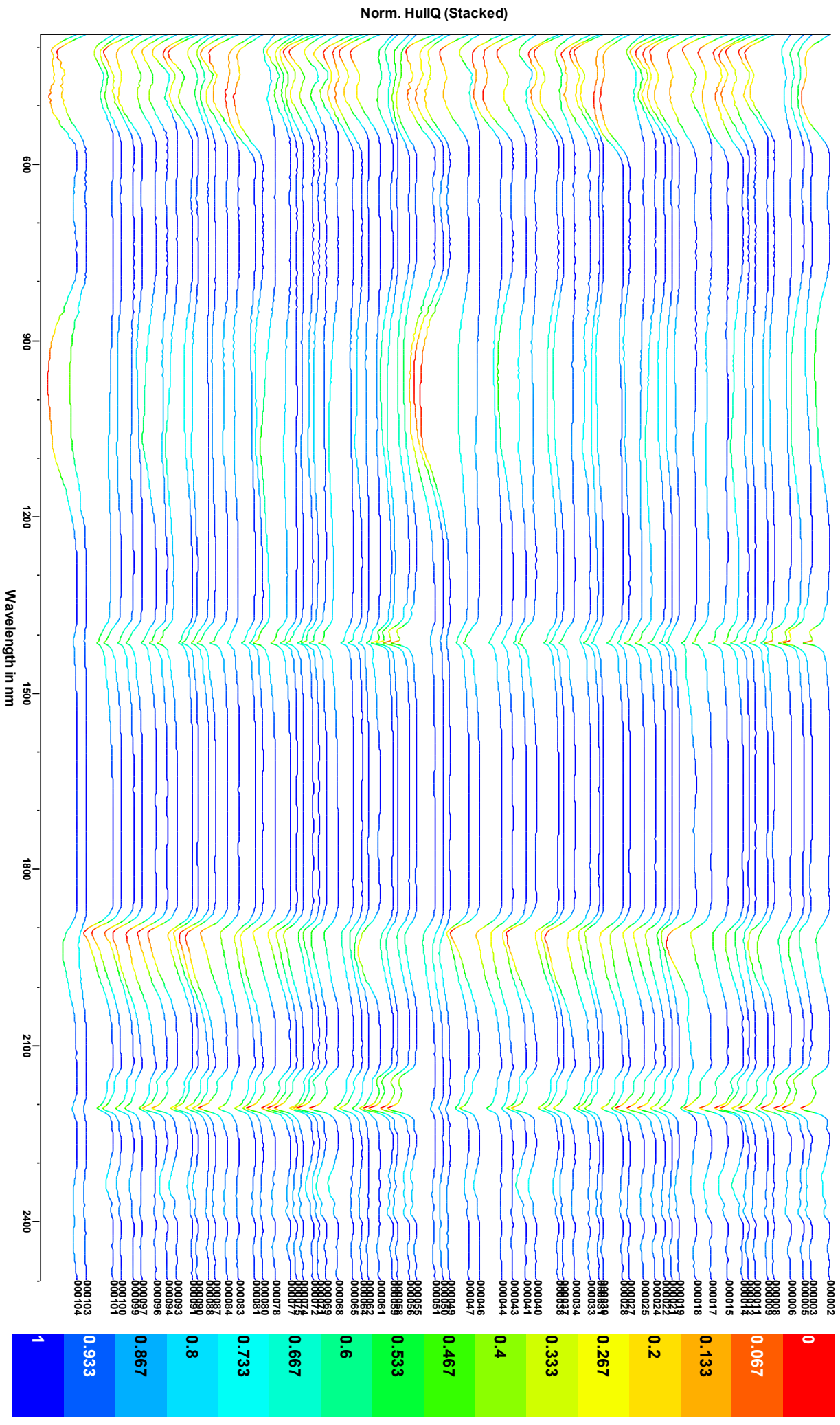
Norm. HullQ (Stacked)
RecorderHill_1_tsgtray, samples 2 to 104 (Aux colour: Norm. HullQ)
Wavelength in nm
600
900
1200
1500
1800
2100
2400
Aux
0
0.067
0.133
0.2
0.267
0.333
0.4
0.467
0.533
0.6
0.667
0.733
0.8
0.867
0.933
1


Recorder Hill
Kaolinite WX
Montmorillonite
Hematite
Gypsum
Muscovite
Siderite
Depth (m)
0.1
0.2
0.3
0.4
0.5
0.6
0.7
0.8
0.9
0
1
0
0.4
0
1
0
0.205
0
0.43
0
0.16

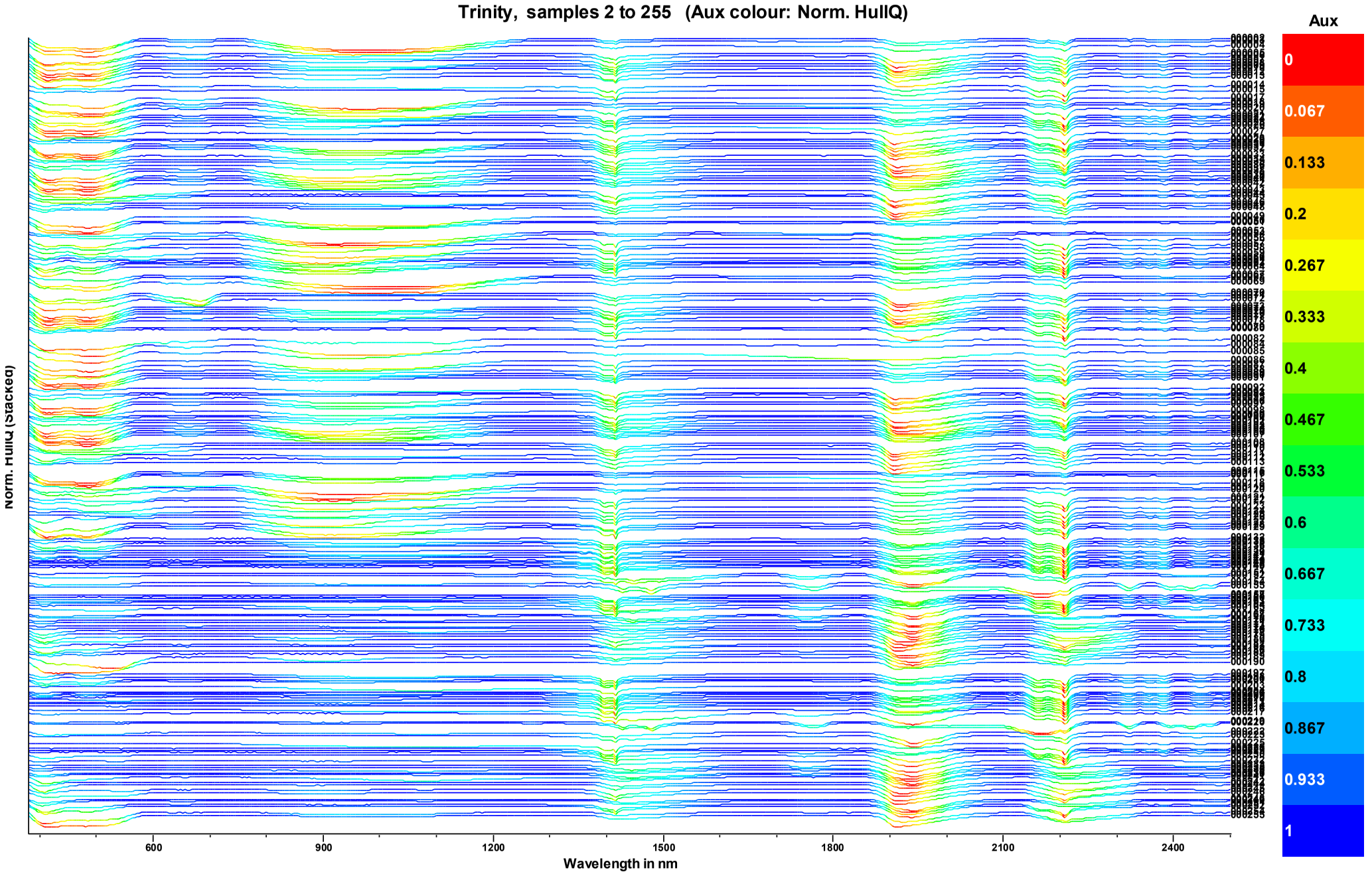
Trinity, samples 2 to 255 (Aux colour: Norm. HullQ)
Aux
0
0.067
0.133
0.2
0.267
0.333
0.4
0.467
0.533
0.6
0.667
0.733
0.8
0.867
0.933
1
Norm. HullQ (Stacked)
600
900
1200
1500
1800
2100
2400
Wavelength in nm

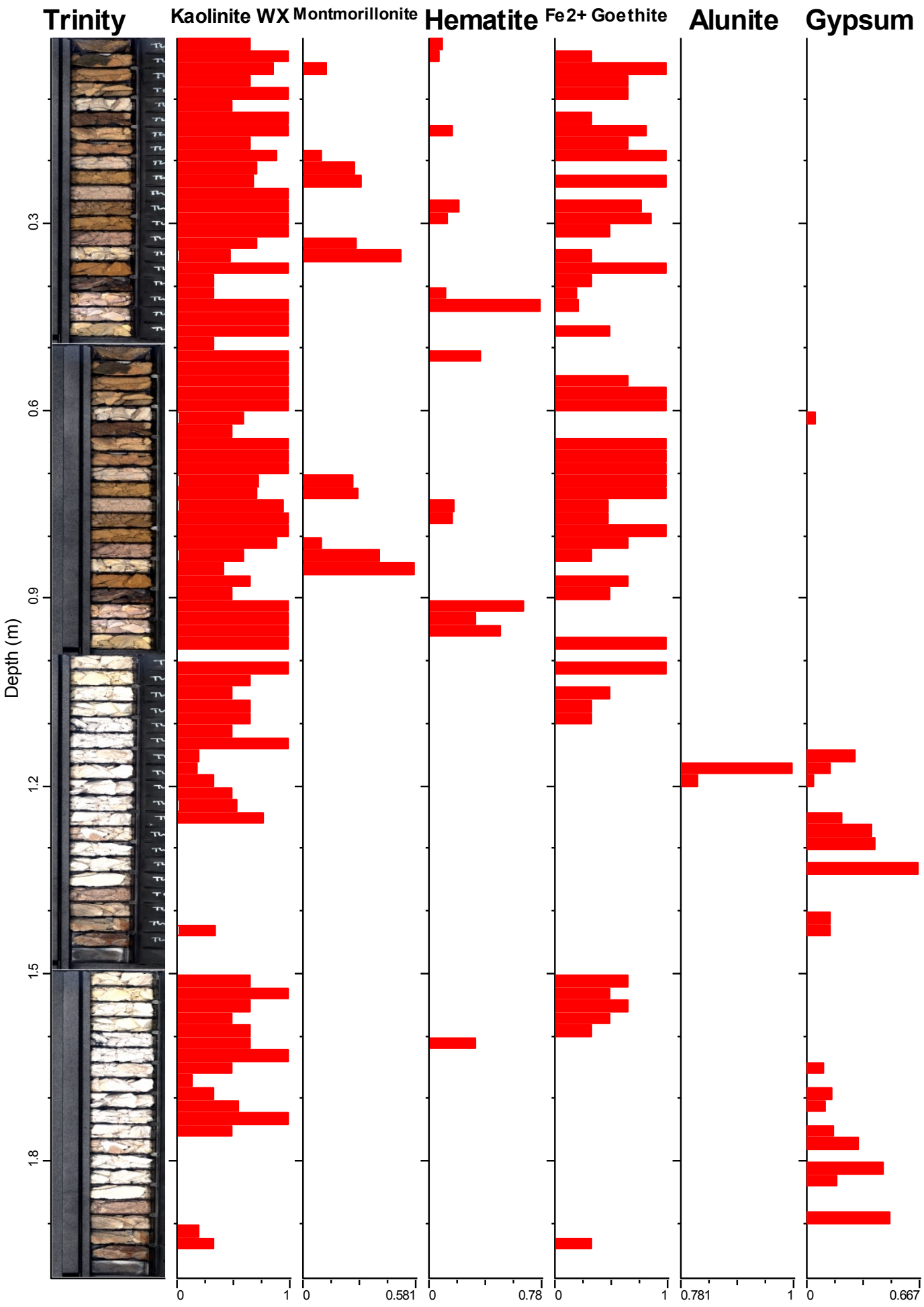
Trinity
Kaolinite WX
Montmorillonite
Hematite
Fe2+ Goethite
Alunite
Gypsum
Depth (m)
0.3
0.6
0.9
1.2
1.5
1.8
0
1
0
0.581
0
0.78
0
1
0.781
1
0
0.667

Appendix 3

Recorder Hill

Concordant Data

Analysis_#	Pb207/U235		Pb206/U238		rho	Concordancy	Age	Error
RH-36-4	0.49178	0.00832	0.06447	0.00092	0.843486	95	402.8	5.58
RH-107-1	0.57109	0.01119	0.07358	0.00112	0.776842	98	457.7	6.7
RH-101-1	0.60522	0.01063	0.0762	0.00115	0.859257	92	473.4	6.88
RH04-70-5	0.6973	0.01147	0.08649	0.00122	0.857532	98	534.8	7.23
RH04-72-1	0.80913	0.01549	0.09581	0.00144	0.785088	91	589.8	8.45
RH-43-1D	1.00352	0.01836	0.11426	0.00172	0.822787	95	697.4	9.92
RH-35-1	1.40987	0.0208	0.14756	0.00194	0.891146	98	887.3	10.92
RH-44-2	1.68883	0.02848	0.16706	0.00248	0.880289	97	1023	27.46
RH04-77-2	1.86434	0.02652	0.17965	0.00237	0.927412	99	1075.9	23.39
RH04-74-3	2.20528	0.03286	0.20221	0.00279	0.925972	101	1174.7	23.54
RH04-72-2	2.20494	0.03726	0.20213	0.00296	0.866592	101	1175.5	27.54
RH-100-2	2.06681	0.03707	0.18883	0.00289	0.853306	94	1182	29.02
RH-98-2	2.0006	0.04123	0.18232	0.00294	0.782456	91	1186.9	35.4
RH-36-2	2.10558	0.03963	0.19093	0.00281	0.781952	94	1196.2	33.25
RH-37-2	2.20006	0.03621	0.19943	0.00266	0.810396	98	1197.4	28.9
RH-41-2	2.2117	0.0413	0.19857	0.00293	0.790187	96	1216.4	30.77
RH-46-2	2.52601	0.03959	0.21693	0.00308	0.905901	97	1303.2	24.29
RH04-73-2	2.34738	0.0371	0.20123	0.00292	0.91812	90	1306.7	24.03
RH04-74-2	3.25429	0.05556	0.25598	0.00391	0.894674	100	1471.8	25.99
RH04-77-1	3.22951	0.04528	0.25284	0.00332	0.936532	98	1480.7	21.82
RH-48-1	3.29942	0.05136	0.25769	0.00361	0.899958	100	1485.1	24.03
RH-35-3	3.37788	0.05089	0.25837	0.00348	0.894023	97	1524.5	23.92
RH-98-1	3.16968	0.05744	0.24099	0.00378	0.865553	91	1536	27.72
RH-95-2	3.57527	0.06285	0.27141	0.00426	0.892868	101	1538.9	25.34
RH04-68-1	3.48274	0.05655	0.26362	0.00389	0.908782	98	1544.4	23.72
RH-103-3	3.56978	0.05938	0.26942	0.004	0.892548	99	1549.6	24.47
RH-107-2	3.3821	0.04946	0.25523	0.00355	0.951106	95	1550.1	21.26
RH-105-2	3.39522	0.06652	0.25567	0.00415	0.828484	94	1554.3	30.08
RH-102-1	3.62265	0.05685	0.27208	0.00403	0.943853	99	1559.3	22.01
RH04-67-1	3.6118	0.05555	0.27029	0.0038	0.914099	99	1565.7	22.86
RH-36-1	3.58551	0.05451	0.26627	0.00369	0.911547	96	1579.7	23.07
RH-52-1	3.60919	0.0591	0.26796	0.00381	0.868315	97	1580.5	25.29
RH-48-3	3.50206	0.05717	0.25742	0.00391	0.930443	92	1599.3	23.02
RH-49-1	3.63383	0.05646	0.2596	0.00382	0.947071	90	1652.3	21.58
RH-96-4	3.88011	0.06635	0.27675	0.00431	0.910737	95	1655.3	23.85
RH-105-1	4.37341	0.07167	0.29705	0.0044	0.90387	96	1746	23.3
RH-50-1	4.36437	0.06868	0.29591	0.00432	0.927717	96	1748.5	22.11
RH-102-2	4.67005	0.07384	0.31242	0.00464	0.93931	99	1773.2	21.72
RH-97-1	4.81072	0.08058	0.31972	0.00494	0.922444	100	1785	23.12
RH-96-1	4.82557	0.08189	0.31685	0.00492	0.915017	98	1807.1	23.36

RH-36-3	4.99876	0.07988	0.32167	0.00463	0.90073	98	1843.1	23.73
RH04-74-1	4.91031	0.08044	0.31201	0.00463	0.905835	94	1866.7	23.51
RH04-68-3	5.93663	0.09008	0.34797	0.00478	0.905311	96	2010.9	21.77
RH-54-1	12.83154	0.20291	0.50045	0.00723	0.913593	97	2706.9	20.63

All data

Analysis_#	Pb207/U235		Pb206/U238		rho	Concordancy	Age	Error
RH-95-1	0.19527	0.0052	0.02718	0.00046	0.635537	60	172.9	2.88
RH-103-2	0.30415	0.00619	0.04023	0.00063	0.769463	63	254.2	3.92
RH-35-2	0.59285	0.00951	0.06439	0.00088	0.851978	48	402.2	5.35
RH-36-4	0.49178	0.00832	0.06447	0.00092	0.843486	95	402.8	5.58
RH-103-1	0.54708	0.01427	0.06459	0.00113	0.670718	62	403.5	6.83
RH-97-3	0.60269	0.01188	0.07349	0.00116	0.800769	78	457.2	6.98
RH-107-1	0.57109	0.01119	0.07358	0.00112	0.776842	98	457.7	6.7
RH-97-2	0.59143	0.01206	0.0743	0.00118	0.778842	89	462	7.08
RH-101-1	0.60522	0.01063	0.0762	0.00115	0.859257	92	473.4	6.88
RH-37-1	0.66233	0.01181	0.07667	0.00109	0.797307	68	476.2	6.5
RH-50-2	0.71183	0.01159	0.0814	0.00118	0.890329	70	504.4	7.05
RH-48-2	0.67253	0.01183	0.08158	0.0012	0.836228	85	505.5	7.16
RH-100-1	0.70716	0.01425	0.08335	0.0013	0.773999	78	516.1	7.71
RH-101-2	0.72128	0.01477	0.08577	0.00134	0.762944	83	530.5	7.93
RH04-70-5	0.6973	0.01147	0.08649	0.00122	0.857532	98	534.8	7.23
RH-4-1D	0.71688	0.01322	0.08677	0.00127	0.793687	89	536.4	7.55
RH-104-1	0.79026	0.01423	0.09302	0.00141	0.841798	87	573.3	8.32
RH-46-3	0.82748	0.01388	0.09307	0.00136	0.871159	76	573.7	8.04
RH04-72-1	0.80913	0.01549	0.09581	0.00144	0.785088	91	589.8	8.45
RH04-70-2	0.93805	0.01494	0.09708	0.0014	0.905469	64	597.2	8.25
RH04-76-3	1.02116	0.01608	0.11217	0.00152	0.860547	85	685.3	8.81
RH-43-1D	1.00352	0.01836	0.11426	0.00172	0.822787	95	697.4	9.92
RH-51-1	1.19342	0.01934	0.12144	0.00178	0.904472	77	738.8	10.22
RH04-70-4	1.25894	0.02617	0.13096	0.00211	0.775077	86	793.3	12.02
RH-35-1	1.40987	0.0208	0.14756	0.00194	0.891146	98	887.3	10.92
RH-44-2	1.68883	0.02848	0.16706	0.00248	0.880289	97	1023	27.46
RH04-77-2	1.86434	0.02652	0.17965	0.00237	0.927412	99	1075.9	23.39
RH-51-2	0.79429	0.01482	0.07546	0.00117	0.830998	42	1104.1	30.96
RH-99-1	0.79841	0.01437	0.07515	0.00115	0.850233	42	1122.8	29.31
RH04-71-1	7.83324	1.5881	0.72163	0.06872	0.469713	301	1165.3	368.21
RH04-74-3	2.20528	0.03286	0.20221	0.00279	0.925972	101	1174.7	23.54
RH04-72-2	2.20494	0.03726	0.20213	0.00296	0.866592	101	1175.5	27.54
RH04-72-3	1.91624	0.03119	0.17514	0.00254	0.891011	88	1181.3	25.83
RH-100-2	2.06681	0.03707	0.18883	0.00289	0.853306	94	1182	29.02
RH-98-2	2.0006	0.04123	0.18232	0.00294	0.782456	91	1186.9	35.4
RH-36-2	2.10558	0.03963	0.19093	0.00281	0.781952	94	1196.2	33.25
RH-37-2	2.20006	0.03621	0.19943	0.00266	0.810396	98	1197.4	28.9
RH-41-2	2.2117	0.0413	0.19857	0.00293	0.790187	96	1216.4	30.77

RH04-70-1	1.97329	0.02896	0.17715	0.00246	0.946207	86	1216.5	22.42
RH-99-2	1.96961	0.0369	0.17488	0.00271	0.827148	84	1238.2	30.68
RH-38-2	2.16435	0.03407	0.19069	0.00256	0.85284	90	1253.3	25.49
RH-99-3	0.93932	0.01553	0.08164	0.00125	0.926081	40	1279.7	24.34
RH-46-2	2.52601	0.03959	0.21693	0.00308	0.905901	97	1303.2	24.29
RH04-73-2	2.34738	0.0371	0.20123	0.00292	0.91812	90	1306.7	24.03
RH-96-3	1.6723	0.02926	0.14254	0.00223	0.894145	65	1317.8	26.25
RH-37-3	2.18171	0.04222	0.18417	0.00284	0.796853	82	1336.9	31.74
RH-106-1	0.68916	0.01211	0.05805	0.00089	0.872497	27	1342.6	27.63
RH04-70-3	1.53325	0.02262	0.12127	0.00169	0.944613	50	1461.2	21.83
RH04-74-2	3.25429	0.05556	0.25598	0.00391	0.894674	100	1471.8	25.99
RH04-77-1	3.22951	0.04528	0.25284	0.00332	0.936532	98	1480.7	21.82
RH-48-1	3.29942	0.05136	0.25769	0.00361	0.899958	100	1485.1	24.03
RH-35-3	3.37788	0.05089	0.25837	0.00348	0.894023	97	1524.5	23.92
RH-98-1	3.16968	0.05744	0.24099	0.00378	0.865553	91	1536	27.72
RH-95-2	3.57527	0.06285	0.27141	0.00426	0.892868	101	1538.9	25.34
RH04-68-1	3.48274	0.05655	0.26362	0.00389	0.908782	98	1544.4	23.72
RH-103-3	3.56978	0.05938	0.26942	0.004	0.892548	99	1549.6	24.47
RH-107-2	3.3821	0.04946	0.25523	0.00355	0.951106	95	1550.1	21.26
RH-105-2	3.39522	0.06652	0.25567	0.00415	0.828484	94	1554.3	30.08
RH-102-1	3.62265	0.05685	0.27208	0.00403	0.943853	99	1559.3	22.01
RH04-67-1	3.6118	0.05555	0.27029	0.0038	0.914099	99	1565.7	22.86
RH-36-1	3.58551	0.05451	0.26627	0.00369	0.911547	96	1579.7	23.07
RH-52-1	3.60919	0.0591	0.26796	0.00381	0.868315	97	1580.5	25.29
RH-48-3	3.50206	0.05717	0.25742	0.00391	0.930443	92	1599.3	23.02
RH-39-1	1.80217	0.0299	0.13039	0.00188	0.869037	49	1628.9	24.86
RH04-69-1	1.52262	0.02538	0.10998	0.00164	0.894602	41	1631.9	24.44
RH04-77-3	2.67448	0.03754	0.19201	0.00253	0.938732	69	1643.3	21.06
RH-49-1	3.63383	0.05646	0.2596	0.00382	0.947071	90	1652.3	21.58
RH-96-4	3.88011	0.06635	0.27675	0.00431	0.910737	95	1655.3	23.85
RH-47-1	0.71118	0.01121	0.04961	0.00071	0.907952	18	1696.5	23.28
RH-106-2	2.59358	0.0402	0.17941	0.00239	0.859458	62	1710.7	24.51
RH-101-3	3.19947	0.05303	0.22035	0.00332	0.909037	75	1720	23.7
RH-105-1	4.37341	0.07167	0.29705	0.0044	0.90387	96	1746	23.3
RH-50-1	4.36437	0.06868	0.29591	0.00432	0.927717	96	1748.5	22.11
RH-102-2	4.67005	0.07384	0.31242	0.00464	0.93931	99	1773.2	21.72
RH-97-1	4.81072	0.08058	0.31972	0.00494	0.922444	100	1785	23.12
RH-96-1	4.82557	0.08189	0.31685	0.00492	0.915017	98	1807.1	23.36
RH04-76-1	3.11482	0.04377	0.2011	0.00266	0.941295	64	1837.9	20.49
RH-36-3	4.99876	0.07988	0.32167	0.00463	0.90073	98	1843.1	23.73
RH04-74-1	4.91031	0.08044	0.31201	0.00463	0.905835	94	1866.7	23.51
RH-40-2	2.914	0.05269	0.18364	0.0027	0.813126	58	1881.6	27
RH-38-1	3.85746	0.05939	0.23906	0.00338	0.918328	72	1911.7	21.51
RH-96-2	4.53146	0.07685	0.27674	0.0043	0.916201	81	1937.8	22.88
RH04-75-2	2.90724	0.04302	0.17689	0.00239	0.913072	54	1944.5	21.48
RH04-76-4	2.58946	0.03742	0.15389	0.00206	0.926323	46	1986.5	20.79

RH04-68-3	5.93663	0.09008	0.34797	0.00478	0.905311	96	2010.9	21.77
RH-34-1	2.85034	0.04197	0.16301	0.00226	0.941568	47	2054.1	20.57
RH-53-1	5.14425	0.08195	0.29023	0.00424	0.917058	79	2078.4	21.75
RH04-75-1	2.44572	0.03618	0.13575	0.00183	0.911275	39	2107.2	21.23
RH-53-2	4.5141	0.07415	0.24716	0.00369	0.908883	67	2131	22.25
RH-39-2	2.93879	0.04956	0.16048	0.00233	0.860939	45	2135.8	23.76
RH-40-1	4.62671	0.08663	0.24654	0.00366	0.792862	65	2178.7	27.32
RH04-76-2	2.12687	0.03003	0.11261	0.00149	0.937119	31	2189.6	19.7
RH04-75-3	0.98188	0.01479	0.05105	0.00069	0.897312	14	2221.3	21.36
RH-46-4	1.0699	0.01708	0.05421	0.00077	0.889747	15	2265.7	22.37
RH-41-1	2.18253	0.03601	0.09271	0.00131	0.85641	22	2565.2	22.62
RH-100-3	0.95952	0.01738	0.04007	0.00063	0.868011	10	2593.7	25.5
RH04-73-1	6.32227	0.09875	0.25859	0.00375	0.928443	56	2628.3	19.96
RH-54-1	12.83154	0.20291	0.50045	0.00723	0.913593	97	2706.9	20.63
RH-49-2	1.0635	0.01616	0.037	0.00053	0.942693	8	2893.7	18.97
RH04-68-2	11.36589	0.17522	0.3657	0.00518	0.918808	67	3019.8	19.35
RH04-71-3	8.96308	0.15536	0.28835	0.00435	0.870337	54	3020.4	22.46
RH-42-2	1.73241	0.03346	0.055	0.00081	0.762513	11	3041.4	26.53
RH-46-1	0.80892	0.01508	0.02547	0.00042	0.884554	5	3054.7	24.93
RH04-71-2	13.88988	0.20618	0.40629	0.00563	0.933521	69	3171.9	18.56

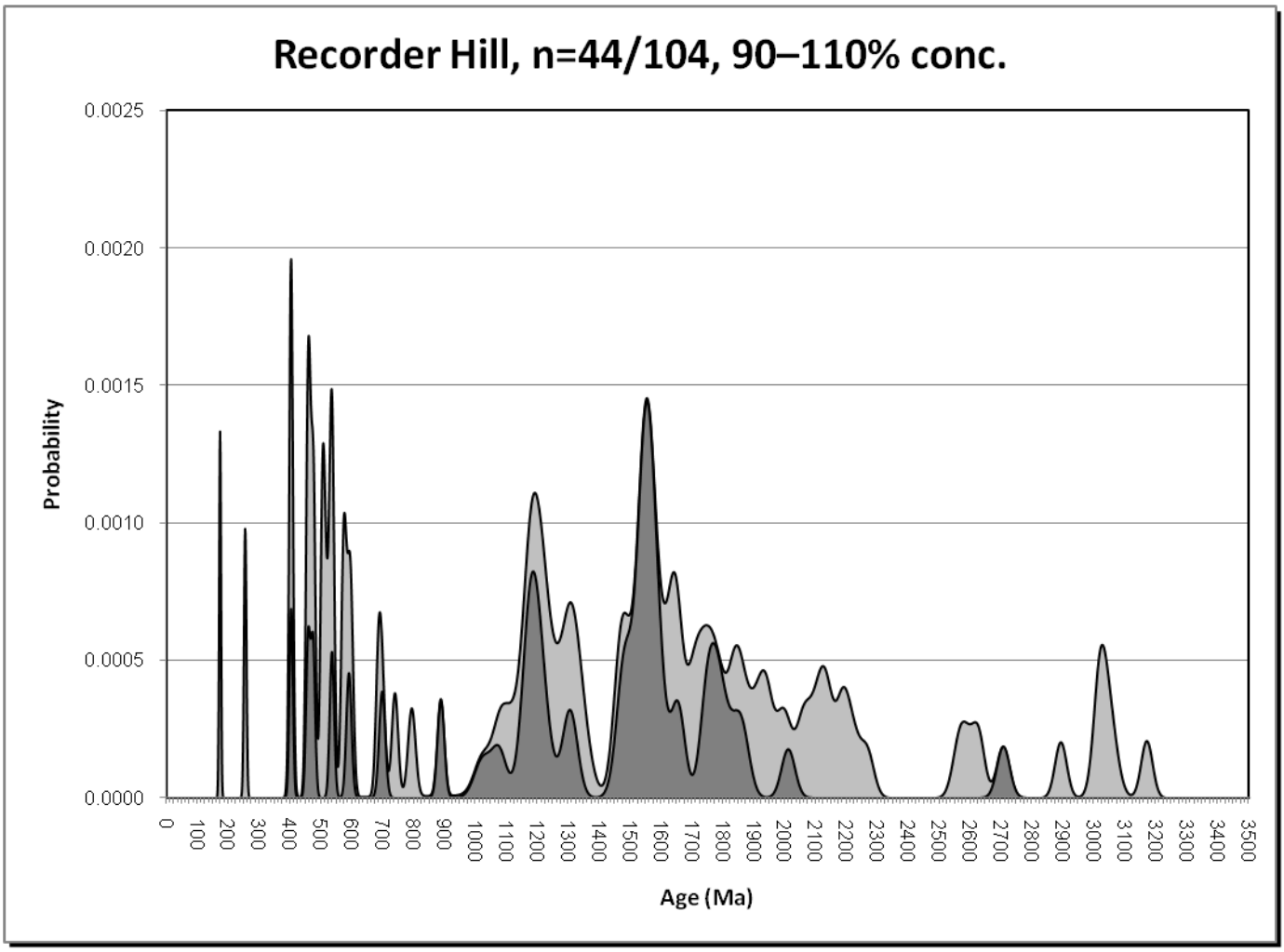

Ludbrook

Concordant Data

Analysis_#	Pb207/U235		Pb206/U238		rho	Concordancy	Age	Error
LUD77-1	0.12751	0.0022	0.01908	0.00025	0.759422	99	121.8	1.58
LUD23-2	0.47995	0.01355	0.06328	0.00088	0.492576	96	395.5	5.35
LUD66-2	0.5158	0.00756	0.06785	0.00084	0.844674	101	423.2	5.06
LUD50-1	0.52027	0.00835	0.06835	0.00089	0.811323	101	426.2	5.38
LUD72-1	0.56978	0.00898	0.07225	0.00095	0.834289	90	449.7	5.7
LUD65-3	0.61373	0.00949	0.07777	0.00097	0.806623	97	482.8	5.79
LUD21-1	0.62448	0.01005	0.07899	0.00089	0.700117	97	490.1	5.32
LUD79-2	0.68318	0.01088	0.08393	0.00107	0.800521	91	519.5	6.36
LUD24-2	0.66222	0.02131	0.08444	0.0012	0.441623	107	522.6	7.15
LUD75-2	0.68145	0.01047	0.08525	0.0011	0.839819	100	527.4	6.52
LUD79-1	0.70782	0.01244	0.08783	0.00115	0.745002	99	542.7	6.84
LUD9-1	1.10273	0.03218	0.12211	0.00188	0.527582	94	742.7	10.79
LUD38-1	1.78232	0.02802	0.17639	0.00203	0.732048	102	1022.5	31.45
LUD75-1	1.80333	0.03077	0.17511	0.00235	0.786511	98	1060.7	31.43
LUD36-1	1.6758	0.03231	0.16197	0.00201	0.643645	90	1070.3	38.8
LUD18-1	1.97277	0.03574	0.18654	0.00228	0.67466	99	1113.4	36.27
LUD64-1	1.96705	0.0293	0.18501	0.00238	0.863634	97	1124.3	26.19
LUD29-1	1.82627	0.04036	0.17165	0.0022	0.579953	91	1125.6	45.13
LUD55-1	2.03418	0.02924	0.18787	0.00238	0.881316	96	1160.5	25.07
LUD23-1	2.06817	0.03526	0.18871	0.00224	0.696237	94	1184.5	33.89
LUD33-1	2.33643	0.04951	0.20869	0.00273	0.617335	100	1227	42.05
LUD66-3	2.28815	0.03648	0.2038	0.00269	0.8279	97	1232	28.05
LUD32-2	2.4121	0.04939	0.21119	0.00273	0.631314	98	1265.8	40.31
LUD15-2	2.41266	0.03985	0.20858	0.00248	0.719858	95	1290.1	32.22
LUD32-3	3.16523	0.0734	0.24348	0.00334	0.591551	93	1514.2	44.97
LUD48-1	3.42606	0.06614	0.26216	0.00325	0.642167	98	1524	37.01
LUD90-1	3.74446	0.05537	0.2854	0.00379	0.898049	106	1531.2	23.46
LUD70-1	3.63343	0.05027	0.27676	0.0035	0.914056	103	1532.5	22.35
LUD34-1	3.43572	0.05699	0.2609	0.00309	0.714009	97	1539	30.99
LUD32-1	3.41709	0.05525	0.25928	0.00302	0.720381	96	1540.3	30.49
LUD65-1	3.62147	0.04658	0.27453	0.0033	0.934565	101	1541.6	21.14
LUD29-2	3.36338	0.05261	0.25483	0.00286	0.717502	95	1542.5	30.18
LUD32-4	3.51946	0.0717	0.26658	0.0034	0.626049	99	1543.8	38.86
LUD14-2	3.39864	0.04566	0.2572	0.00291	0.842154	96	1544.8	24.27
LUD72-4	3.5877	0.05085	0.27117	0.00338	0.879428	100	1547.2	23.72
LUD88-1	3.41277	0.0456	0.25784	0.00328	0.952063	96	1547.7	20.79
LUD51-1	3.6807	0.0494	0.27804	0.00356	0.953995	102	1548	20.74
LUD65-4	3.69406	0.04887	0.27901	0.00344	0.931966	102	1548.5	21.37
LUD45-2	3.52722	0.05529	0.26616	0.00307	0.735837	98	1550.4	29.41
LUD25-3	3.48068	0.06599	0.26227	0.00326	0.655624	97	1552.8	36.62
LUD19-2	3.32818	0.04874	0.25052	0.00285	0.776826	93	1555	27.45

LUD88-3	3.4804	0.04784	0.26186	0.00331	0.919595	96	1555.6	22.04
LUD71-2	3.6251	0.04728	0.2726	0.00332	0.933802	100	1556.6	21.35
LUD83-2	3.73019	0.05436	0.28043	0.00369	0.902929	102	1557.3	23.07
LUD65-6	3.56804	0.05017	0.268	0.00325	0.862451	98	1558.9	24.01
LUD82-1	3.56335	0.05102	0.26763	0.00348	0.90816	98	1559	22.72
LUD18-2	3.59531	0.05017	0.27002	0.00309	0.820077	99	1559.1	25.57
LUD60-1	3.70524	0.05912	0.27826	0.00365	0.822099	101	1559.6	27.08
LUD83-1	3.76929	0.0521	0.2829	0.00362	0.925758	103	1560.1	21.83
LUD88-2	3.72059	0.05161	0.27796	0.00362	0.938867	101	1568.7	21.36
LUD71-3	3.75568	0.05001	0.27978	0.00344	0.923365	101	1574.2	21.63
LUD80-1	3.66638	0.05263	0.27271	0.00347	0.886406	99	1577	23.47
LUD28-1	3.69607	0.07787	0.27349	0.00369	0.640405	98	1587.1	39.91
LUD68-2	3.78021	0.05489	0.27963	0.00359	0.884165	100	1587.4	23.66
LUD74-2	3.91595	0.05263	0.28858	0.0036	0.928197	102	1594.7	21.45
LUD28-2	3.60804	0.07001	0.26578	0.00332	0.643765	95	1595.3	36.57
LUD61-1	3.68077	0.06313	0.26417	0.00359	0.792344	92	1644.2	29.04
LUD40-1	4.24083	0.07936	0.28739	0.0036	0.669391	93	1749.9	35.06
LUD25-1	4.5976	0.08094	0.31086	0.00391	0.714463	99	1754.1	32.25
LUD55-2	4.61411	0.06375	0.30752	0.00398	0.936737	97	1779.7	20.86
LUD52-1	5.19634	0.07072	0.33469	0.0043	0.94402	101	1841.9	20.38
LUD52-2	5.25285	0.0699	0.33347	0.00416	0.937464	99	1868.2	20.48
LUD38-2	5.77882	0.11681	0.34479	0.00449	0.644245	96	1979.7	36.1

All data;

Analysis_#	Pb207/U235		Pb206/U238		rho	Concordancy	Age	Error
LUD25-2	0.12411	0.01264	0.01883	0.00055	0.286795	134	120.2	3.48
LUD77-1	0.12751	0.0022	0.01908	0.00025	0.759422	99	121.8	1.58
LUD20-1	0.13608	0.00552	0.01958	0.00029	0.365124	59	125	1.84
LUD89-1	0.13688	0.00331	0.01954	0.00028	0.592578	54	124.8	1.76
LUD74-1	0.13842	0.00374	0.01935	0.00029	0.554682	44	123.5	1.86
LUD23-2	0.47995	0.01355	0.06328	0.00088	0.492576	96	395.5	5.35
LUD66-2	0.5158	0.00756	0.06785	0.00084	0.844674	101	423.2	5.06
LUD50-1	0.52027	0.00835	0.06835	0.00089	0.811323	101	426.2	5.38
LUD19-1	0.46665	0.01367	0.06041	0.00088	0.497275	83	378.1	5.34
LUD24-2	0.66222	0.02131	0.08444	0.0012	0.441623	107	522.6	7.15
LUD29-3	0.51796	0.01467	0.06597	0.00092	0.492388	84	411.8	5.55
LUD72-1	0.56978	0.00898	0.07225	0.00095	0.834289	90	449.7	5.7
LUD65-3	0.61373	0.00949	0.07777	0.00097	0.806623	97	482.8	5.79
LUD21-1	0.62448	0.01005	0.07899	0.00089	0.700117	97	490.1	5.32
LUD72-2	0.56773	0.0115	0.07147	0.00099	0.683841	86	445	5.97
LUD75-2	0.68145	0.01047	0.08525	0.0011	0.839819	100	527.4	6.52
LUD79-1	0.70782	0.01244	0.08783	0.00115	0.745002	99	542.7	6.84
LUD15-1	0.54636	0.01325	0.06777	0.00092	0.559775	77	422.7	5.54
LUD13-1	0.63076	0.02124	0.07751	0.00119	0.455931	85	481.2	7.11
LUD79-2	0.68318	0.01088	0.08393	0.00107	0.800521	91	519.5	6.36
LUD60-2	0.68909	0.01147	0.0842	0.00104	0.742051	90	521.1	6.2

LUD48-2	0.54843	0.02222	0.06651	0.00111	0.41192	70	415.1	6.71
LUD85-1	0.67413	0.00995	0.08172	0.00106	0.878816	85	506.4	6.32
LUD12-1	0.60382	0.01299	0.07319	0.00092	0.584298	76	455.3	5.52
LUD35-1	0.68972	0.02329	0.08309	0.00132	0.470466	84	514.6	7.89
LUD62-1	0.64014	0.00901	0.07614	0.00094	0.877132	74	473	5.65
LUD67-1	0.68157	0.01064	0.08014	0.00101	0.807311	75	497	6.06
LUD65-2	0.80179	0.01227	0.09247	0.00118	0.833868	81	570.1	6.98
LUD66-1	0.21714	0.00885	0.02496	0.00045	0.442348	22	158.9	2.82
LUD51-2	0.17701	0.00516	0.02033	0.00032	0.539959	18	129.8	2
LUD46-1	0.68902	0.01621	0.07797	0.00102	0.55606	65	484	6.08
LUD86-1	0.54174	0.00875	0.06084	0.00082	0.834464	50	380.7	5.01
LUD9-1	1.10273	0.03218	0.12211	0.00188	0.527582	94	742.7	10.79
LUD11-1	0.95384	0.06417	0.09954	0.00239	0.356898	67	611.7	14.03
LUD62-2	0.66025	0.00919	0.06672	0.00084	0.904516	42	416.3	5.07
LUD38-1	1.78232	0.02802	0.17639	0.00203	0.732048	102	1022.5	31.45
LUD14-1	1.32272	0.02287	0.1303	0.00156	0.69244	77	1031.5	34.92
LUD75-1	1.80333	0.03077	0.17511	0.00235	0.786511	98	1060.7	31.43
LUD36-1	1.6758	0.03231	0.16197	0.00201	0.643645	90	1070.3	38.8
LUD67-2	0.56701	0.00778	0.05442	0.00067	0.897279	32	1083.7	24.2
LUD18-1	1.97277	0.03574	0.18654	0.00228	0.67466	99	1113.4	36.27
LUD64-1	1.96705	0.0293	0.18501	0.00238	0.863634	97	1124.3	26.19
LUD29-1	1.82627	0.04036	0.17165	0.0022	0.579953	91	1125.6	45.13
LUD55-1	2.03418	0.02924	0.18787	0.00238	0.881316	96	1160.5	25.07
LUD10-1	0.63707	0.00884	0.05865	0.00066	0.810981	31	1167	26.75
LUD56-1	1.2184	0.01673	0.11177	0.00142	0.925246	58	1173.8	22.94
LUD23-1	2.06817	0.03526	0.18871	0.00224	0.696237	94	1184.5	33.89
LUD33-1	2.33643	0.04951	0.20869	0.00273	0.617335	100	1227	42.05
LUD66-3	2.28815	0.03648	0.2038	0.00269	0.8279	97	1232	28.05
LUD11-2	0.52135	0.00762	0.04574	0.00052	0.777824	23	1261.7	28.07
LUD32-2	2.4121	0.04939	0.21119	0.00273	0.631314	98	1265.8	40.31
LUD67-3	1.8713	0.02549	0.16184	0.00201	0.911767	75	1289.5	23.2
LUD15-2	2.41266	0.03985	0.20858	0.00248	0.719858	95	1290.1	32.22
LUD32-3	3.16523	0.0734	0.24348	0.00334	0.591551	93	1514.2	44.97
LUD48-1	3.42606	0.06614	0.26216	0.00325	0.642167	98	1524	37.01
LUD90-1	3.74446	0.05537	0.2854	0.00379	0.898049	106	1531.2	23.46
LUD70-1	3.63343	0.05027	0.27676	0.0035	0.914056	103	1532.5	22.35
LUD11-3	3.12441	0.04541	0.23736	0.00275	0.797153	89	1538.1	26.55
LUD34-1	3.43572	0.05699	0.2609	0.00309	0.714009	97	1539	30.99
LUD32-1	3.41709	0.05525	0.25928	0.00302	0.720381	96	1540.3	30.49
LUD65-1	3.62147	0.04658	0.27453	0.0033	0.934565	101	1541.6	21.14
LUD29-2	3.36338	0.05261	0.25483	0.00286	0.717502	95	1542.5	30.18
LUD32-4	3.51946	0.0717	0.26658	0.0034	0.626049	99	1543.8	38.86
LUD14-2	3.39864	0.04566	0.2572	0.00291	0.842154	96	1544.8	24.27
LUD72-4	3.5877	0.05085	0.27117	0.00338	0.879428	100	1547.2	23.72
LUD88-1	3.41277	0.0456	0.25784	0.00328	0.952063	96	1547.7	20.79
LUD51-1	3.6807	0.0494	0.27804	0.00356	0.953995	102	1548	20.74

LUD65-4	3.69406	0.04887	0.27901	0.00344	0.931966	102	1548.5	21.37
LUD16-1	4.38456	0.06849	0.33117	0.00384	0.742299	119	1549	29.34
LUD45-2	3.52722	0.05529	0.26616	0.00307	0.735837	98	1550.4	29.41
LUD61-2	3.08523	0.04812	0.23263	0.00304	0.837857	87	1552.2	26.17
LUD25-3	3.48068	0.06599	0.26227	0.00326	0.655624	97	1552.8	36.62
LUD19-2	3.32818	0.04874	0.25052	0.00285	0.776826	93	1555	27.45
LUD88-3	3.4804	0.04784	0.26186	0.00331	0.919595	96	1555.6	22.04
LUD71-2	3.6251	0.04728	0.2726	0.00332	0.933802	100	1556.6	21.35
LUD83-2	3.73019	0.05436	0.28043	0.00369	0.902929	102	1557.3	23.07
LUD65-6	3.56804	0.05017	0.268	0.00325	0.862451	98	1558.9	24.01
LUD82-1	3.56335	0.05102	0.26763	0.00348	0.90816	98	1559	22.72
LUD18-2	3.59531	0.05017	0.27002	0.00309	0.820077	99	1559.1	25.57
LUD60-1	3.70524	0.05912	0.27826	0.00365	0.822099	101	1559.6	27.08
LUD83-1	3.76929	0.0521	0.2829	0.00362	0.925758	103	1560.1	21.83
LUD88-2	3.72059	0.05161	0.27796	0.00362	0.938867	101	1568.7	21.36
LUD71-3	3.75568	0.05001	0.27978	0.00344	0.923365	101	1574.2	21.63
LUD80-1	3.66638	0.05263	0.27271	0.00347	0.886406	99	1577	23.47
LUD28-1	3.69607	0.07787	0.27349	0.00369	0.640405	98	1587.1	39.91
LUD68-2	3.78021	0.05489	0.27963	0.00359	0.884165	100	1587.4	23.66
LUD74-2	3.91595	0.05263	0.28858	0.0036	0.928197	102	1594.7	21.45
LUD28-2	3.60804	0.07001	0.26578	0.00332	0.643765	95	1595.3	36.57
LUD18-3	3.17945	0.0481	0.23325	0.00263	0.745317	84	1603.2	28.57
LUD65-5	2.61148	0.03562	0.19089	0.00236	0.906404	70	1609.8	22.23
LUD41-1	2.49293	0.0382	0.18188	0.00206	0.739144	67	1613.6	28.69
LUD61-1	3.68077	0.06313	0.26417	0.00359	0.792344	92	1644.2	29.04
LUD57-1	2.76337	0.03803	0.1949	0.00239	0.891043	68	1676.1	22.68
LUD40-1	4.24083	0.07936	0.28739	0.0036	0.669391	93	1749.9	35.06
LUD25-1	4.5976	0.08094	0.31086	0.00391	0.714463	99	1754.1	32.25
LUD68-1	1.77519	0.02317	0.11884	0.00145	0.934812	41	1771.8	20.58
LUD55-2	4.61411	0.06375	0.30752	0.00398	0.936737	97	1779.7	20.86
LUD45-1	2.75979	0.04152	0.18087	0.00203	0.746016	59	1810.8	27.51
LUD13-2	3.82279	0.05638	0.24764	0.00283	0.774856	78	1831.8	26.6
LUD52-1	5.19634	0.07072	0.33469	0.0043	0.94402	101	1841.9	20.38
LUD52-2	5.25285	0.0699	0.33347	0.00416	0.937464	99	1868.2	20.48
LUD38-2	5.77882	0.11681	0.34479	0.00449	0.644245	96	1979.7	36.1
LUD72-3	3.41029	0.49059	0.191	0.01019	0.370863	54	2087.6	246.44
LUD30-1	6.14296	0.09026	0.33053	0.00369	0.759797	85	2161.7	26.06
LUD63-1	9.01005	0.12512	0.43889	0.00544	0.892573	111	2333.5	21.11
LUD71-1	9.45141	0.1183	0.44003	0.00528	0.958658	88	2410.4	18.35
LUD24-1	12.33507	0.20719	0.3909	0.00483	0.735621	70	3044.5	26.35

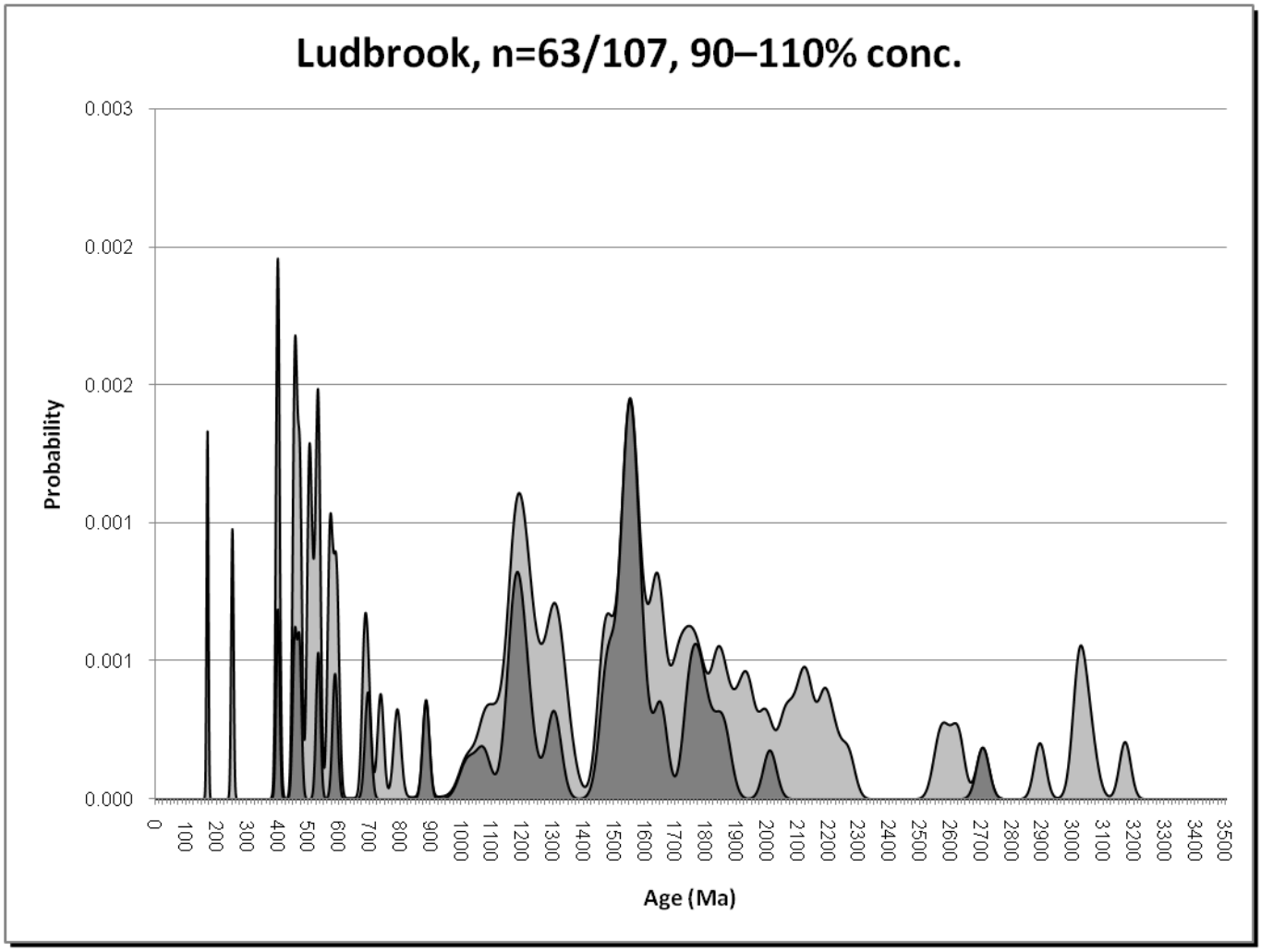
Ludbrook, n=63/107, 90–110% conc.
Probability
0.003
0.002
0.002
0.001
0.001
0.000
0
100
200
300
400
500
600
700
800
900
1000
1100
1200
1300
1400
1500
1600
1700
1800
1900
2000
2100
2200
2300
2400
2500
2600
2700
2800
2900
3000
3100
3200
3300
3400
3500
Age (Ma)